Differentially expressed circular RNAs in peripheral blood mononuclear cells of PD patients

Stylianos Ravanidis[1], Anastasia Bougea[1,2,3], Dimitra Karampatsi[1], Nikolaos Papagiannakis[2,3], Matina Maniati[2], Leonidas Stefanis[2,3], Epaminondas Doxakis MSc[1]

Centers of [1] Basic Research and [2] Clinical Research, Biomedical Research Foundation, Academy of Athens, Athens, 11527, Greece.

[3] First Department of Neurology, National and Kapodistrian University of Athens Medical School, Athens, 11528, Greece.

Corresponding author: Epaminondas Doxakis

Corresponding author's address: Center of Basic Research, Biomedical Research Foundation, Academy of Athens, Soranou Efesiou 4, Athens, 11527, Greece.

Corresponding author's phone +30-2106597479, Fax: +30-2106597545

Corresponding author's e-mail address: edoxakis@bioacademy.gr

ABSTRACT

Background

New noninvasive and affordable molecular approaches that will complement current practices and increase the accuracy of PD diagnosis are urgently needed. CircRNAs are highly stable non-coding RNAs that accumulate with aging in neurons and are increasingly shown to regulate all aspects of neuronal development and function.

Objectives

The aims of the present study were to identify differentially expressed circRNAs in PBMCs of idiopathic PD patients and explore the competing endogenous RNA networks affected.

Methods

Eighty-seven circRNAs were initially selected based on relatively high gene expression in the human brain. Over half of these were readily detectable in PBMCs using RT-qPCR. Comparative expression analysis was then performed in PBMCs from sixty controls and sixty idiopathic subjects with PD.

Results

Six circRNAs derived from MAPK9, HOMER1, SLAIN1, DOP1B, REPS1, and PSEN1 transcripts were significantly downregulated in PD patients. The classifier that best distinguished PD consisted of four circRNAs with an AUC of 0.84. CLIP-Seq data revealed that the RNA binding proteins bound by most of the deregulated circRNAs include the neurodegeneration-associated FUS, TDP43, FMR1 and ATXN2. MicroRNAs predicted to be sequestered by most deregulated circRNAs had the GOslim categories ‘Protein modification’, ‘Transcription factor activity’ and ‘Cytoskeletal protein binding’ mostly enriched.

Conclusions

This is the first study that identifies circRNAs deregulated in the peripheral blood of PD patients. They may serve as diagnostic biomarkers and since they are highly expressed in the brain and are derived from genes with essential brain functions, they may also hint on the PD pathways affected.

INTRODUCTION

The diagnosis of PD is currently based on clinical diagnostic criteria and neuroimaging and is monitored by rating scales related to motor and non-motor features [1]. Rating scales are frequently subjective and influenced by periodic fluctuations in symptoms and effective symptomatic therapies, while neuroimaging techniques, such as DAT-SPECT, offer a quantifiable measure of disease progression but are limited by practicality and costs [2]. In addition, protein biomarkers, such as those based on alpha-synuclein (SNCA) and dopamine metabolic products have yielded mixed results, do not reflect disease progression and require an invasive lumbar puncture [3].

Circular RNAs (circRNAs) are a newly recognized class of single-stranded regulatory RNAs that are formed by head-to-tail splicing in which a downstream 5' splice site is covalently connected to an upstream 3' splice site of an RNA molecule. The result is an enclosed non-polyadenylated circular transcript [4-6]. Due to the lack of free ends, that are normally targeted by 3' and 5' exoribonucleases, circRNAs are extremely stable with half-life of more than 48 h compared to approximately 6 h of linear transcripts [7, 8]. There are different subtypes of circRNAs including exonic, intronic and exo-intronic. Exonic circRNAs are mostly localized in the cytoplasm where they act as sponges for microRNAs (miRNAs) and RNA-binding proteins (RBPs), thus inhibiting their interaction with mRNA targets [4, 9-11]. In contrast, intronic or exo-intronic circRNAs are mostly localized in the nucleus and have few or no binding sites for miRNAs; instead they function to control transcription [12, 13]. Interestingly, the co-transcriptional biogenesis of circRNAs has also

been shown to reduce linear host mRNA levels and change downstream splice-site choice in some mRNAs [11, 14, 15].

CircRNAs are widely conserved and more abundant in the brain than in any other tissue [16] with many being expressed in an organ-specific manner, along with their host genes which are enriched with tissue-specific biological functions [17]. For instance, brain circRNA host genes are enriched in neurotransmitter secretion, synaptic activities and neuron maturation [17]. Importantly, however, they are regulated independently from their linear counterparts [16, 18] with 60% of CNS circRNAs being upregulated throughout development, especially during synaptogenesis, while only 2% of their linear isoforms show this tendency [17].

Recent studies revealed the deregulation of circRNAs in neurodegenerative diseases and neuropsychiatric disorders (reviewed in [19]). Furthermore, several brain-enriched circRNAs have been associated with pathogenetic processes of neurodegeneration. For instance, CDR1as (ciRS-7), a highly abundant circRNA in the brain, is downregulated in the brain of patients with AD [20]. This circRNA contains 63 binding sites for miR-7 and therefore it is acting as an efficient sponge for it [4]. Importantly, critical proteins for the neurodegeneration processes such as the ubiquitin protein ligase A (UBE2A), which catalyses the proteolytic clearing of toxic amyloid peptides in AD, and SNCA, which accumulates in PD/AD, are both targets of miR-7 [21, 22]. More recently, another circRNA, circSLC8A1, was found to increase in the substantia nigra of individuals with PD and in cultured cells exposed to the oxidative stress-inducing agent paraquat [23]. Importantly, circSLC8A1 carries seven binding sites for miR-128, an abundant and brain-restricted miRNA that governs neuronal excitability and motor behavior [24-27].

Peripheral blood mononuclear cells (PBMCs) inherit the same genetic information as brain cells and are armed with abundant signaling pathways that respond to pathological changes. Multiple

studies have shown that genome-wide transcriptional and alternative splicing profiles in peripheral blood parallel changes in gene expression in the brain, reflecting broad molecular and cellular impairments [28-33]. Therefore, PBMCs provide a powerful and minimally-invasive tool for the identification of novel targets for neurodegeneration research. Considering that circRNAs a) are abundant in the brain modulating gene expression *en masse*, b) are stable, c) do not get modified like proteins, hence levels directly correlate with activity and d) can be accurately quantified by routine and fast laboratory methods, such as RT-qPCR, suggests that they not only represent excellent candidate biomarkers but also important constituents of the pathophysiological processes implicated in neurological diseases. The purpose of this study was to identify differentially expressed brain-enriched circRNAs in PBMCs from patients with idiopathic PD (iPD) and pinpoint competing endogenous (ceRNA) networks.

MATERIAL AND METHODS

Figure 1 provides a schematic representation of the workflow.

Study population

The present study included 60 iPD patients and 60 healthy individuals in two separate cohorts. Patients were assessed with brain magnetic resonance imaging (MRI) or computed tomography (CT) and no relevant brain vascular lesions explaining the clinical phenotype were detected. The control group included spouses or unrelated companions of patients who had no known neurological disease, comorbidities or PD family history. Individuals with concurrent malignant tumours, psychiatric disorders, collagen diseases, endocrine and cardiovascular diseases, or infections were excluded from this study, since these conditions are expected to alter the

expression profile of transcripts. Patients affected by atypical parkinsonism were also excluded. All patients and controls were recruited from the National and Kapodistrian University of Athens' First Department of Neurology at Eginition hospital. PD was diagnosed by two neurologists according to Postuma et al., criteria [1]. In all cases, essential demographic and clinical information, including the study questionnaire for motor and non-motor manifestations of the disease, rating scales [Hoehn & Yahr (H&Y) stage, mini-mental state examination (MMSE, cognitive impairment score <26 [34]), Unified Parkinson's Disease Rating Scale part III (UPDRS III) in the on or off state] were collected and documented. The demographic and clinical features of patients and controls are summarized in Table 1. Levodopa equivalent daily dose (LEDD) was calculated for the patient group according to Tomlinson et al., criteria [35]. The Eginition hospital and BRFAA ethics committees approved the study and all participants provided written consent.

Isolation of peripheral blood mononuclear cells

PBMCs were isolated from whole blood by employing density-gradient centrifugation using the Biocoll Separating Solution according to manufacturer's instructions (Biochrom AG).

Total RNA extraction and RT-qPCR analysis

Total RNA extraction was performed using the RNAzol®-RT reagent according to manufacturer's instructions (Molecular Research Center, MRC). To improve the yield of the small RNA fraction, a polyacryl carrier (PC152, MRC) was added during the extraction method. Reverse transcription reactions were performed in triplicate for every sample. Similarly, qPCR was performed in triplicate on the Roche Lightcycler® 96 using the SYBR FAST Universal 2X qPCR Master Mix from Kapa Biosystems. For the differential expression analysis, we selected only those circRNAs

that were detected in PBMCs with a crossing threshold (Ct) value below 30, for improved detection accuracy. All primers span the splice junction. *U6* and *GAPDH* were used as reference genes. The relative expression level of circRNAs was calculated using the $2^{-\Delta\Delta Ct}$ method between age- and gender- matched counterparts. Primer sequences can be found in Suppl. Table 1.

CircRNA selection process

Eighty-seven circRNAs were carefully selected by cross-examining the data from three genome-wide surveys [4, 18, 36]. We chose circRNAs that had high expression in the brain (Rybak-Wolf score above ~1,000) and low or no expression in other tissues. The host gene expression was also taken into account in the selection process. Initially, based on GTEx portal expression data, circRNAs for which host transcripts were specifically expressed in the brain were selected. However, we found that many circRNAs derived from these transcripts were not readily detectable in PBMCs. We, therefore, widened the analysis to host transcripts that are brain- or at least cerebellum-enriched (i.e. not exclusively expressed in the brain). Last, we included six brain-abundant circRNAs deriving from host transcripts with low expression in the brain (UBXN7_circ_0001380, TMEM138_circ_0002058, ZNF292_circ_0004058, HAT1_circ_0008032, ZFAND6_circ_0000643, UIMC1_circ_0001558) and eight circRNAs that are hosted by brain-relevant transcripts that have been found deregulated in AD (CORO1C_circ_0000437, WDR78_circ_0006677, PHC3_circ_0001359, SLAIN2_circ_0126525) [37] and autism (FAM120A_circ_0001875, CSNK1G3_circ_0001522, VMP1_circ_0006508, SMARCA5_circ_0001445) [38]. For the list of circRNAs analyzed see Suppl. Tables 1 and 2.

CircRNA target network

The interactions of the differentially expressed circRNAs with miRNAs and RBPs were identified by obtaining data from the Circular RNA Interactome (CircInteractome) and Interactional Database of Cancer-Specific CircRNAs (IDCSC) databases, respectively [39, 40]. CircInteractome utilizes the TargetScan algorithm to predict microRNA response elements (MREs, ie miRNA-binding sites) while IDCSC hosts circRNA cross-linking immunoprecipitation (CLIP)-Seq data for the different RBPs extracted from StarBase database [41]. The circRNA-miRNA and circRNA-RBP interactomes were then manually curated using the Cytoscape v.3.8.0 platform.

miRNA pathway analysis

The DIANA mirPath v.3 software suite was used to identify miRNA-regulated pathways. This software renders possible the functional annotation of miRNAs using standard hypergeometric distributions, unbiased empirical distributions and meta-analysis statistics [42]. Here, predicted targets from DIANA microT-CDS algorithm with high quality experimentally supported interactions were used to identify KEGG molecular pathways, as well as GO terms targeted by each miRNA. The combinatorial effect of deregulated miRNAs was identified by simultaneously selecting multiple miRNAs in the software. The default values (p-value threshold 0.05, microT-CDS threshold 0.8, FDR correction option ticked) were used for the analysis.

Statistical analysis

Statistical analysis was performed using GraphPad PRISM v5.0 and R v3.5.3. All data underwent a normality test (Shapiro–Wilk), and were found to be non-normally distributed. As a result, all circRNA data underwent a logarithmic transformation (with base 2), in order to better approximate the normal distribution. The parametric t-test was used to observe differences between healthy

controls and PD patients. We applied the Benjamini – Hochberg false discovery rate correction in the resulting p-values to account for the multiple number of tests. Spearman's method with Bonferroni correction for multiple comparisons was used to correlate circRNA expression levels with participants' demographic and clinical characteristics (p-value threshold 0.0005).

To assess the possibility that sex is a confounding factor, the two-way ANOVA model was applied to the log-transformed data (normally distributed) with sex as an additional factor. No difference in the circRNAs that were statistically significant was found.

Receiver operating characteristic (ROC) curves were constructed and the area under the curve (AUC) was calculated to evaluate the predictive sensitivity and specificity of PBMC circRNAs for PD diagnosis. The cutoff value for the ROC analysis was determined using the Youden Index. Data are presented as means ± SEM. circRNA selection was based on the stepwise removal approach. A logistic regression statistical model containing all available circRNAs as independent variables and PD status as the dependent variable was built. Then, the circRNAs with the least contribution in the model (as determined by an F test) were removed. This process continued until no further removals were possible.

Data availability

The datasets analysed during the current study are all available from the corresponding author on request.

RESULTS

circRNAs are differentially expressed in PBMCs of idiopathic PD patients

The demographic and clinical characteristics of 60 healthy controls and 60 iPD patients are summarized in Table 1. The mean age of 64.5 and the sex ratio were the same for both groups. The disease duration for the PD group was 4.8±0.55 years and the MMSE score 27.5±0.56. Initially, RT-qPCR was employed to detect plasma levels of 32 circRNAs that are highly-expressed by brain cells. It was anticipated that a sufficient quantity of brain-derived circRNAs would find its way into the plasma. However, only two circRNAs, RMST (at Ct 29) and PSD3 (at Ct 28), were detected. Using the same amount of RNA, this time extracted from human brain tissue, it was revealed that all circRNAs were readily detectable with an average Ct value of 26, demonstrating that all primer pairs were functional (data not shown). This indicated that brain-enriched circRNAs are not as abundant as brain-enriched miRNAs (average Ct value of 17.5 for 21 brain-enriched miRNAs in the same human brain total RNA) and are not circulating in appreciable amount in the blood (average Ct value for the corresponding miRNAs in the plasma is 25) [43].

Based on previous studies showing that genome-wide transcriptional and alternative splicing profiles in peripheral blood cells parallel changes in gene expression in the brain, the levels of circRNAs were next assessed in PBMCs. We increased the number of primer sets to 87 and found that 48 were detected with a Ct value below 30, safeguarding accurate and reproducible detection. These circRNAs were then analyzed for differential expression in healthy control and iPD patient samples (Suppl. Table 3).

Following multiple comparison adjustment, six circRNAs were significantly altered in the PBMCs obtained from PD patients compared to healthy controls. MAPK9_circ_0001566, HOMER1_circ_0006916, SLAIN1_circ_0000497, DOP1B_circ_0001187, RESP1_circ_0004368, and PSEN1_circ_0003848 were all downregulated in the PD cohort (Fig.

2 and Suppl. Table 3). The swarm plots for the 42 circRNAs whose relative expression was not significantly altered in the PBMCs of idiopathic PD patients are shown in Supplemental Fig 1.

Association between circRNA levels and clinical features, age or sex

Spearman correlation test was used to relate circRNA levels to iPD patients' clinical features. We found no correlation between age-at-onset, disease duration, UPDRS III, MMSE, LEDD, H&Y or patients' on/off state and circRNA levels (Suppl. Table 4 and data not shown). Finally, correcting clinical scores with LEDD did not reveal any more associations (data not shown). In addition, there was no significant correlation between circRNA expression and age or sex in either healthy controls or PD patients.

Discriminant Analysis

To evaluate the utility of PBMC circRNA levels in discriminating subjects with iPD from healthy controls, ROC curve analysis was performed. The diagnostic sensitivity and specificity of a four circRNA panel (SLAIN1_circ_0000497, SLAIN2_circ_0126525, ANKRD12_circ_0000826, and PSEN1_circ_0003848) were 75.3% (62.1-85.2%) and 78% (65.8-88%), respectively, and the AUC was 0.84 (Fig. 3).

CeRNA networks

CircRNAs can act as miRNA and RBP sponges for regulating gene expression. To explore the functional role of the deregulated circRNAs we identified all their miRNA and RBP targets. Multiple miRNA binding sites are predicted for each circRNA, with SLAIN1_circ_0000497 and MAPK9_circ_0001566 having the most of MREs (38 and 24, respectively) (Fig. 4A).

Interestingly, five miRNAs were predicted to be sponged by half or more of the deregulated PD circRNAs. miR-526b and miR-659 are the top targets, sequestered by four deregulated PD circRNAs (Fig. 4A). Fig. 4B shows the deregulated circRNA-RBP network. Like for miRNAs, CLIP-Seq data obtained from StarBase database revealed that the deregulated circRNAs have multiple RBP binding sites. MAPK9_circ_0001566 and HOMER1_circ_0006916 host the most of these sites with 60 and 49 sites, respectively. Interestingly, 29 RBPs were sequestered by four or more deregulated circRNAs.

CircRNA-miRNA pathway analysis

In order to explore the biological pathways affected by the five miRNAs (miR-516b-5p, miR-526b-5p, miR-578, miR-659-3p, and miR-1197) mostly sequestered by three or more of the deregulated circRNAs, the DIANA mirPath v3 tool was used to align miRNA predicted targets with KEGG pathways and GOslim categories. A Priori gene union analysis of deregulated miRNA targets revealed fourteen KEGG categories as significantly enriched; they included 'Thyroid hormone signaling pathway' ($p < 0.0015$, 24 genes), 'Regulation of actin cytoskeleton' ($p < 0.015$, 42 genes) 'Phosphatidylinositol signaling pathway' ($p < 0.016$, 16 genes), 'MAPK signaling pathway' ($p < 0.016$, 46 genes) and 'FoxO signaling pathway' ($p < 0.016$, 26 genes) (Suppl. Table 5A). Similar findings were obtained using a Posteriori analysis (Suppl. Fig. 2A). Thirty-nine GOslim categories that are controlled by the gene union of the deregulated miRNA targets were enriched following a Priori analysis; these included 'Cellular protein modification' ($p < 3.93E-19$, 283 genes), 'Nucleic acid binding transcription factor activity' ($p < 7.74E-07$, 112 genes), 'Cytoskeletal protein binding' ($p < 3.91E-09$, 102 genes) 'Cell death' ($p < 7.91E-08$, 112 genes),

'RNA binding' ($p< 6.93E-07$, 207 genes) and 'Response to stress' ($p< 3.72E-05$, 225 genes) (Suppl. Table 5B). Similar findings were obtained using a Posteriori analysis (Suppl. Fig. 2B).

DISCUSSION

We profiled brain-enriched circRNAs in peripheral blood from controls and patients with PD using a RT-qPCR -based approach for three reasons. First, primers could be designed to span the splicing junction which guarantees that only message from the circRNA is amplified. Second, RT-qPCR is the most sensitive method to accurately determine expression changes between cohorts; the alternative microarray approach is prone to errors at multiple levels and nearly always requires a follow up RT-qPCR-based analysis to validate findings. Third, we probed circRNAs that are abundantly expressed in the brain; in this way, we could identify differentially expressed or spliced circRNAs that are more likely associated with the neurological processes of PD.

Insights into the differentially expressed circRNA genes

We initiated our study with 87 brain-enriched circRNAs from which over half were confidently detected in PBMCs. From these circRNAs, six were differentially expressed in PD with a 17% decrease on average from healthy controls levels. These changes may appear subtle but depending on the circRNA baseline expression levels and considering the relative importance of their multiple targets (transcription factors, RBPs, and miRNAs) as well as the added-up deregulation of the common targets, the biological outcome is expected to be significant.

It has been observed that the biological role of host transcripts reflects on the function of the circRNAs [17]. We found that the host transcripts of the differentially-expressed circRNAs are not exclusive to brain pathways; rather, they are house-keeping genes, whose functions are best

characterized in the CNS as they are essential for neuronal homeostasis. A brief bibliographical overview of their properties is described below.

Hsa_circ_0001566 is hosted by the mitogen-activated protein kinase 9 (MAPK9) gene. MAPK9/JNK2 is a member of the c-Jun n-terminal kinase 1-3 family robustly activated by environmental stresses, including the PD-related neurotoxins lipopolysaccharides (LPS), MPTP and 6-hydroxydopamine (6-OHDA) to mediate neuronal degeneration [44]. It is indispensable during brain development for neuronal migration, axonal sprouting and guidance, as well as neuronal survival [45]. Hsa_circ_0006916 is hosted by the homer scaffold protein 1 (HOMER1) gene. HOMER1 is a member of Homer 1-3 family constituting important scaffold proteins at the postsynaptic density that associate with a large number of Ca^{2+}-handling proteins, including channels, receptors, and shank scaffolding proteins to regulate intracellular Ca^{2+} homeostasis [46]. An SNP in the promoter of HOMER1 has been associated with psychotic symptoms in PD [47]. Further, circHomer1a is reduced in the prefrontal cortex of patients with schizophrenia and bipolar disorder, where it modulates the alternative splicing of mRNA transcripts involved in synaptic plasticity and psychiatric disease [11]. Hsa_circ_0000497 is hosted by the SLAIN motif family member 1 (SLAIN1) gene. SLAIN1 and 2 are microtubule-associated proteins that promote persistent microtubule growth by recruiting the microtubule polymerase ch-TOG to microtubule plus-ends and thus they are important for axon elongation in developing neurons [48]. Recently, SLAIN1 was identified as a candidate gene for intellectual disability [49]. Hsa_circ_0001187 is hosted by the DOP1 leucine zipper like protein B (DOP1B) gene. DOP1B/ DOPEY2/ C21orf5 and its ortholog DOP1A interact with partner MON2 to retrograde transport endosomes from the TGN to the Golgi [50, 51]. DOP1B is a candidate gene for mental retardation in Down syndrome [52, 53] and copy number variations (CNVs) have been observed in AD [54, 55]. Hsa_circ_0004368 is hosted by

the RALBP1 associated eps domain containing 1 (REPS1) gene. REPS1 is a signaling and endocytosis adaptor that interacts with adaptor Intersectin 1 (ITSN1) in clathrin-coated pits and Amphiphysin 1 (AMPH) at the surface of synaptic vesicles [56]. Mutations in REPS1 are associated with neurodegeneration with brain iron accumulation (NBIA) in the basal ganglia [57]. Hsa_circ_0003848 is hosted by the presenilin 1 (PSEN1) gene. PSEN1 and its paralog PSEN2 are the endoprotease subunits of the gamma-secretase complex that catalyses the intramembrane cleavage of integral membrane proteins such as Notch receptors and amyloid-beta precursor protein (APP). Mutations in either gene cause early-onset AD [58] and α-synuclein accumulation in LB in these patients [59]. Besides their established role in mediating the formation of Aβ peptide, more recently mutant PS1 has been shown to impair numerous cellular functions such as calcium flux, organization of proteins in different compartments, and protein turnover via vacuolar metabolism [60]. Interestingly, a novel PSEN1 mutation was recently identified as the likely cause for early-onset Parkinsonism [61].

Correlation between circRNA levels and demographics

There was no significant correlation between the differential expression of a particular circRNA and clinical or demographic measures. Combined interactions with age and sex did not also appear to affect circRNA levels. These findings reinforce current knowledge that the etiology of PD is complex involving a mix of genetic and environmental influences on ageing brain. Similar findings have been observed in miRNA studies [62]. Further, a pool of four circRNAs discriminated subject with PD from controls with an AUC of 0.84.

CircRNA-RBP and circRNA-miR interactions

In silico approaches were utilized to identify potential biological roles for the deregulated circRNAs by identifying the RBPs and miRNAs that are sequestered preferentially by them. Since

the circRNAs were all downregulated, it indicates that target RBP and miRNA functions will be enhanced in PD. The circRNA-RBP network which is based on experimental CLIPS-seq data revealed that 29 RBPs were bound by four or more deregulated circRNAs. Importantly, several of these RBPs are implicated in familial neurodegeneration including Fragile X Mental Retardation Protein 1 (FMR1, Fragile X syndrome and associated disorders), Ataxin 2 (ATXN2, Spinocerebellar ataxia 2, late-onset PD), Fused in Sarcoma (FUS) and TAR DNA binding protein (TARDBP/TDP43) (Amyotrophic lateral sclerosis, Frontotemporal dementia) [63-72].

The circRNA-miRNA network revealed five miRNAs that were predicted to be sponged by at least three downregulated PD circRNAs. miR-659-3p is of particular interest as it targets progranulin (PGRN), a neuroprotective and anti-inflammatory protein implicated in FTD [73-77]. To explore the molecular pathways controlled by the five miRNAs, *in silico* analysis of KEGG pathways and GOslim terms was performed. KEGG categories revealed multiple signaling pathways (Thyroid hormone, Phosphatidylinositol, MAPK, FoxO) implicated in neuronal survival and plasticity and 'Regulation of actin cytoskeleton' which is central to pre- and postsynaptic assembly as over-represented [78-81]. GOslim analysis revealed 'Cellular protein modification', 'Nucleic acid binding transcription factor activity', 'Cytoskeletal protein binding', 'Cell death', and 'Response to stress' as overrepresented among the biological processes affected. 'Cellular protein modifications' such as phosphorylation, ubiquitination, truncation, acetylation, nitration and sumoylation of PD-linked proteins have emerged as important modulators of pathogenic mechanisms in PD [82, 83]. 'Transcription factor' changes indicate that there is not only misexpression at the mRNA translation level by miRNA deregulation, but that there exists a second wave of *en masse* deregulation involving transcription-mediated changes. Finally, deregulation of fine cytoskeletal dynamics is expected to impair trafficking and intracellular signaling pathways and has been

recognized as a key insult in the pathogenesis of multiple neurodegenerative diseases including PD [84, 85].

Conclusions

We performed an RT-qPCR-based analysis on RNA extracted from PBMC cells from a cohort of patients with PD and matched controls to identify deregulated circRNAs. The circRNAs investigated are highly-expressed in the human brain. This is the first study of its kind in PD. The measurement of four out of six downregulated circRNAs provided reasonable sensitivity and specificity for PD in this discovery cohort. The circRNAs found deregulated form a robust set of brain-associated circRNAs, that can now be further evaluated, along with other measures, as diagnostic and possible therapeutic targets for PD. *In silico* analysis provided a comprehensive guide of the pathways and processes they control, shedding light on their potential biological role. The impact of these findings will now await further exploration.

ABBREVIATIONS

6-OHDA, 6-hydroxydopamine; ANCOVA, analysis of covariance; ANOVA, analysis of variance; APP, amyloid-beta precursor protein; AUC, area under the curve; circRNA, circular RNA; CT, computed tomography; DOP1B, DOP1 leucine zipper like protein; FTD, Frontotemporal dementia; GO, gene ontology; H&Y, Hoehn & Yahr; HC, healthy control; HDAC, histone deacetylase; HOMER1, homer scaffold protein 1; hsa, homo sapiens; iPD, idiopathic PD; KEGG, Kyoto encyclopedia of genes and genomes; LEDD, Levodopa equivalent daily dose; LPS, lipopolysaccharides; MAPK9, mitogen-activated protein kinase 9; MMSE, Mini Mental State Examination; MRI, magnetic resonance imaging; NBIA, neurodegeneration with brain iron accumulation; PD, Parkinson's disease; PSEN1, presenilin 1; REPS1, RALBP1 associated eps

domain containing 1; SNCA, alpha-synuclein; SLAIN1, SLAIN motif family member; UPDRS, unified Parkinson's disease rating scale; TARDBP, TAR DNA Binding Protein; UTR, untranslated region.

ACKNOWLEDGMENTS

The authors are grateful to patients, relatives, and volunteer healthy controls for their participation in this study. This research was financed by Greece and European Union (European Social Fund-ESF) through the Operational Program «Human Resources Development, Education and Lifelong Learning 2014-2020» in the context of the project "Development of diagnostic biomarker tests for Parkinson's disease" (MIS 5049385). It was also co-financed by the action "Precision medicine Hellenic network in genetic neurodegenerative diseases" (2018ΣΕ01300001) of the Hellenic public investments program of GSRT and the Michael J. Fox Foundation for Parkinson's Research (Grant ID 13353).

AUTHORS' ROLES

Conceived the study: ED. Neurologically examined patients: AB, NP, LS. Peripheral blood processing: MM. Differential expression analysis: SR, DK, ED. Analyzed data: SR, NP, ED. Bioinformatics analyses: ED. Wrote the manuscript: ED. All authors read, edited and approved the final manuscript.

FINANCIAL DISCLOSURES

Stylianos Ravanidis: SR is a postdoctoral researcher at BRFAA. No Disclosures.

Anastasia Bougea: AB is a neurology resident at Eginition Hospital. No Disclosures.

Dimitra Karampatsi: DK is a former MSc student at BRFAA. No Disclosures.

Nikolaos Papagiannakis: NP is a neurology resident at Eginition Hospital. No Disclosures.

Matina Maniati: MM is a technician at BRFAA. No Disclosures.

Leonidas Stefanis: Leonidas Stefanis is employed by the National and Kapodistrian University of Athens and the Biomedical Research Foundation of the Academy of Athens. He has the following active grants: Fondation Sante research grant, a Michael J. Fox Foundation grant as a collaborator and an ELIDEK grant. He has served on an Advisory Board for Abbvie, Novartis and Roche and has received honoraria from Abbvie and Sanofi.

Epaminondas Doxakis: ED is employed by BRFAA. He has one active MJFF research grant.

FIGURES

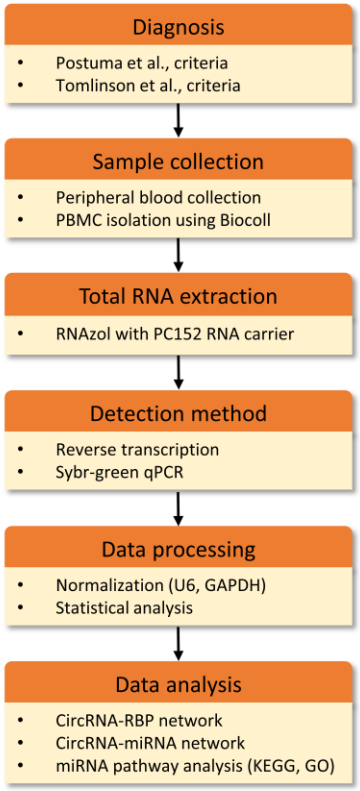

Figure 1. Schematic representation of the workflow.

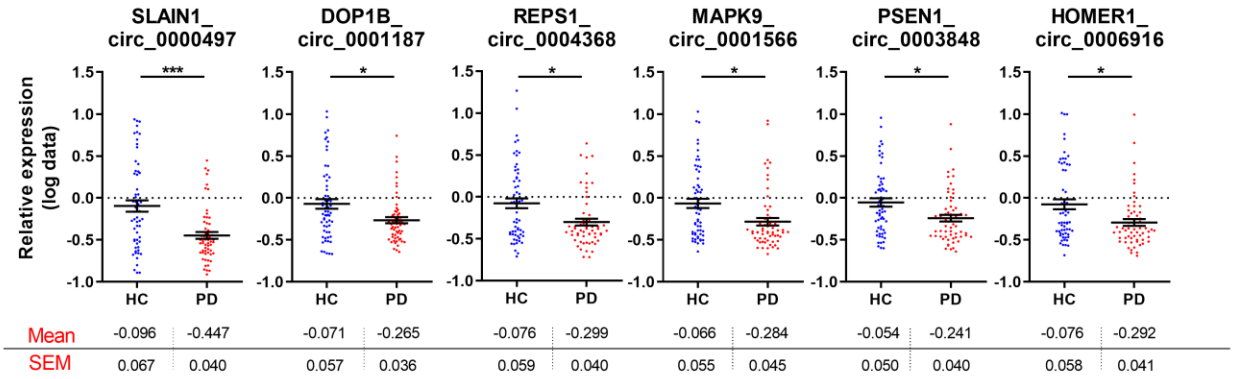

Figure 2. Swarm plots of deregulated circRNAs relative expression in the PBMCs of control and idiopathic PD cohorts. Mean levels +/- SEM are included below each graph. Graphs demonstrate relative expression of log-transformed data. Unpaired t-test was used to determine the significance of differences between the two groups. *p<0.05, **p<0.01, ***p<0.001.

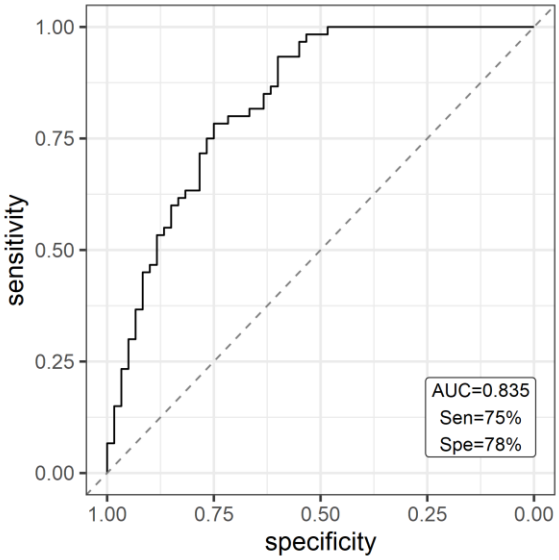

Figure 3. The receiver operating characteristic (ROC) curve analysis for discriminating idiopathic PD from healthy control subjects. ROC curve of four circRNAs (MAPK9_circ_0001566, SLAIN1_circ_0000497, SLAIN2_circ_0126525, and PSEN1_circ_0003848) differentiate iPD from HC cases.

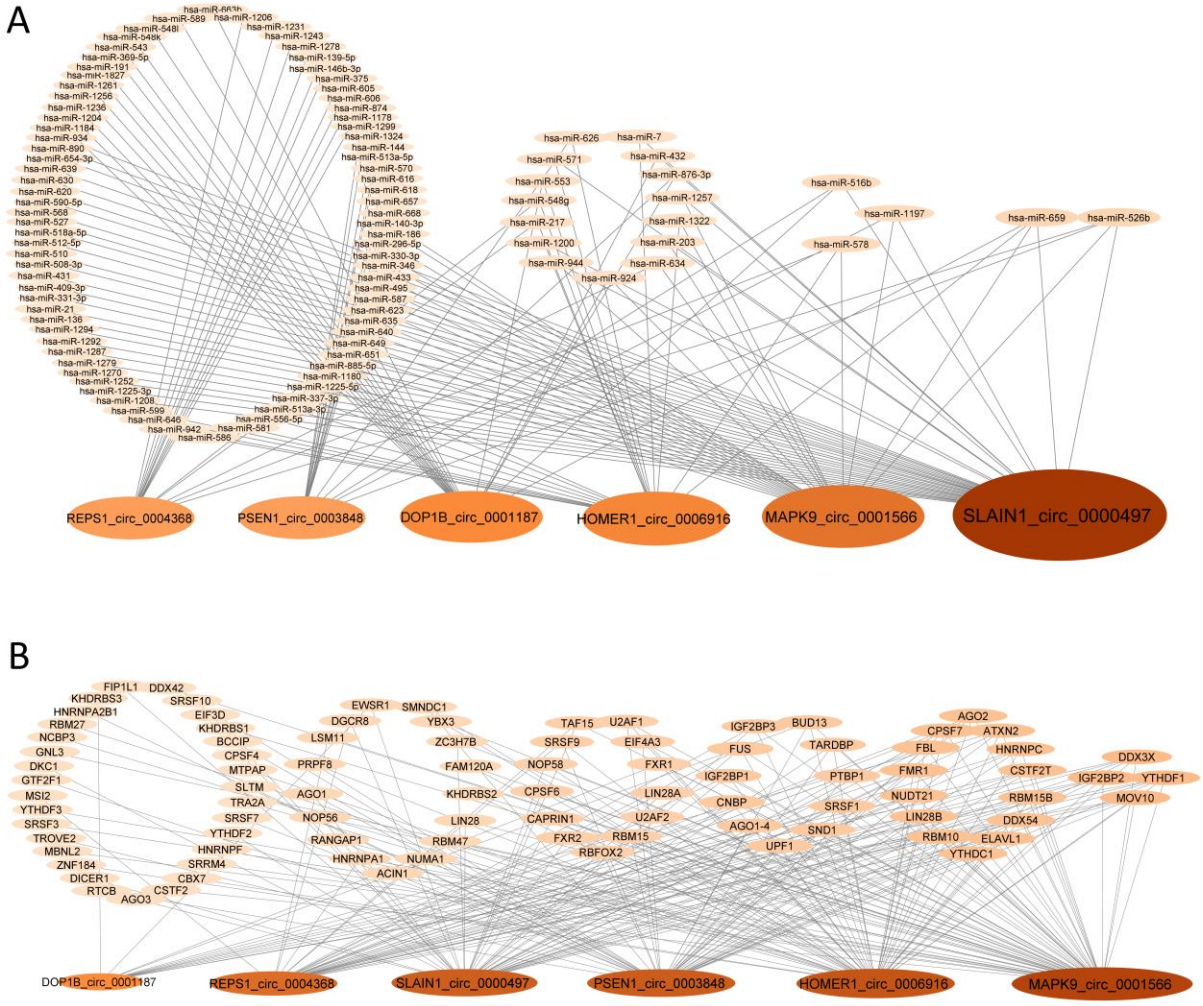

431

432 **Figure 4. CircRNA target networks.** Diagrams show (A) the predicted miRNAs and (B) the

433 CLIP-Seq identified RBPs that bind to differentially expressed circRNAs.

434

435

SUPPLEMENTAL FIGURES

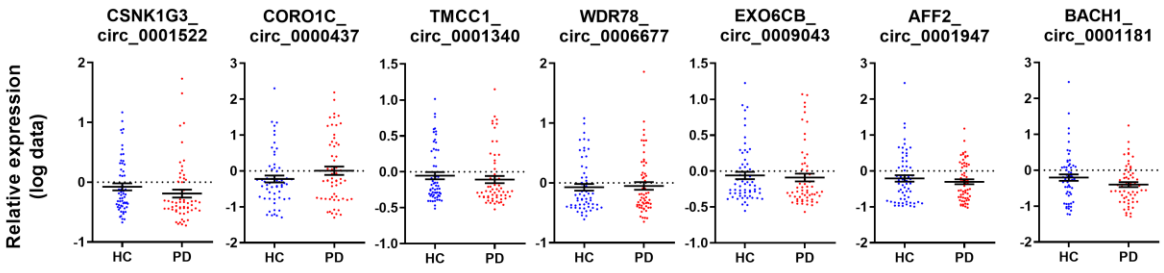

	CSNK1G3_ circ_0001522		CORO1C_ circ_0000437		TMCC1_ circ_0001340		WDR78_ circ_0006677		EXO6CB_ circ_0009043		AFF2_ circ_0001947		BACH1_ circ_0001181	
Mean	-0.077	-0.190	-0.224	0.007	-0.054	-0.108	-0.072	-0.051	-0.061	-0.089	-0.208	-0.302	-0.203	-0.399
SEM	0.059	0.066	0.095	0.118	0.049	0.051	0.057	0.064	0.051	0.055	0.091	0.069	0.089	0.070

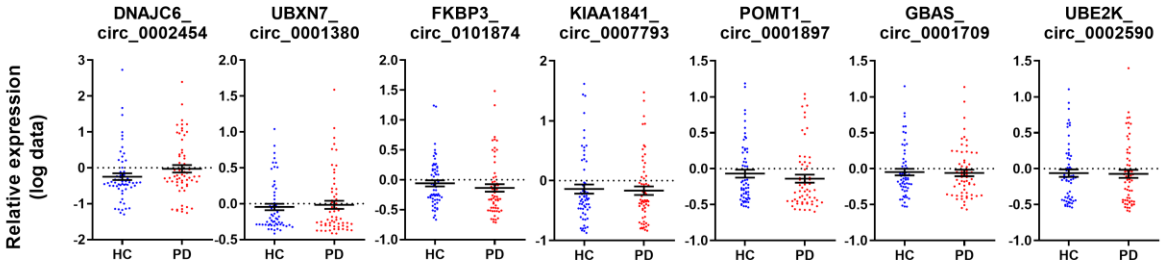

	DNAJC6_ circ_0002454		UBXN7_ circ_0001380		FKBP3_ circ_0101874		KIAA1841_ circ_0007793		POMT1_ circ_0001897		GBAS_ circ_0001709		UBE2K_ circ_0002590	
Mean	-0.247	-0.027	-0.046	-0.016	-0.059	-0.136	-0.141	-0.168	-0.069	-0.139	-0.047	-0.060	-0.062	-0.073
SEM	0.094	0.104	0.045	0.056	0.051	0.063	0.076	0.072	0.055	0.057	0.046	0.046	0.053	0.056

437

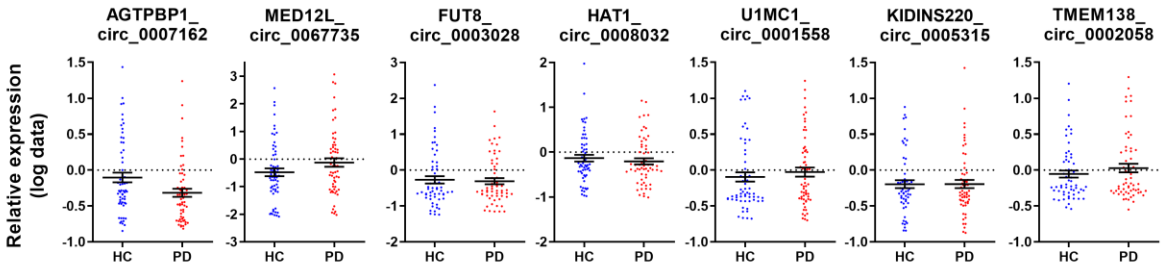

	AGTPBP1_ circ_0007162		MED12L_ circ_0067735		FUT8_ circ_0003028		HAT1_ circ_0008032		U1MC1_ circ_0001558		KIDINS220_ circ_0005315		TMEM138_ circ_0002058	
Mean	-0.103	-0.317	-0.477	-0.124	-0.270	-0.309	-0.133	-0.204	-0.095	0.028	-0.149	-0.194	-0.055	0.028
SEM	0.068	0.056	0.142	0.155	0.102	0.084	0.075	0.068	0.064	0.064	0.072	0.057	0.049	0.060

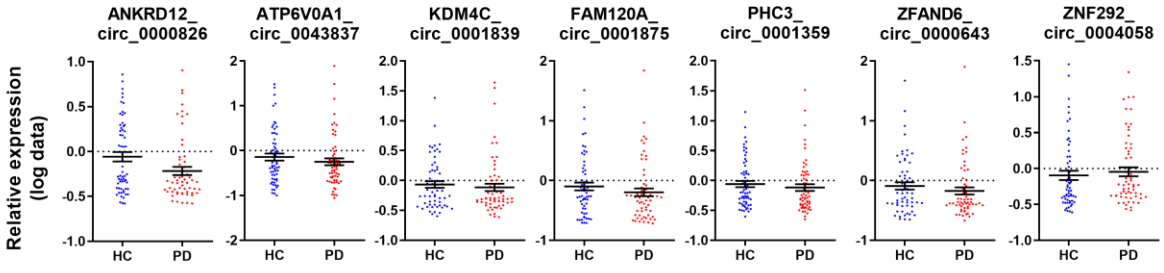

	ANKRD12_ circ_0000826		ATP6V0A1_ circ_0043837		KDM4C_ circ_0001839		FAM120A_ circ_0001875		PHC3_ circ_0001359		ZFAND6_ circ_0000643		ZNF292_ circ_0004058	
Mean	-0.059	-0.217	-0.142	-0.250	-0.066	-0.115	-0.098	-0.196	-0.060	-0.118	-0.090	-0.173	-0.095	-0.045
SEM	0.052	0.046	0.079	0.077	0.054	0.062	0.065	0.065	0.052	0.056	0.062	0.063	0.064	0.062

438

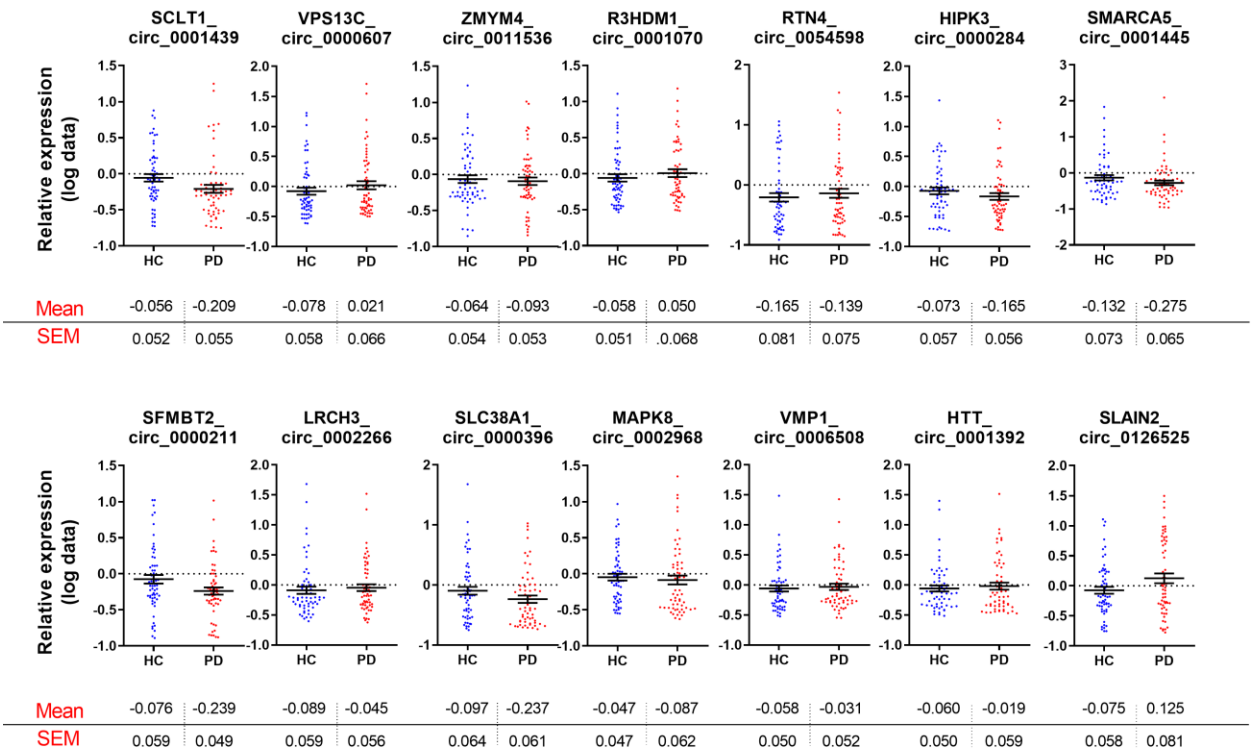

Supplemental Figure 1. Swarm plots for the 42 circRNAs whose relative expression is not significantly altered in the PBMCs of idiopathic PD patients. Mean levels +/- SEM are included below each graph. Graphs demonstrate relative expression of log-transformed data. Unpaired t-test was used to determine the significance of differences between the two groups. *p<0.05, **p<0.01, ***p<0.001.

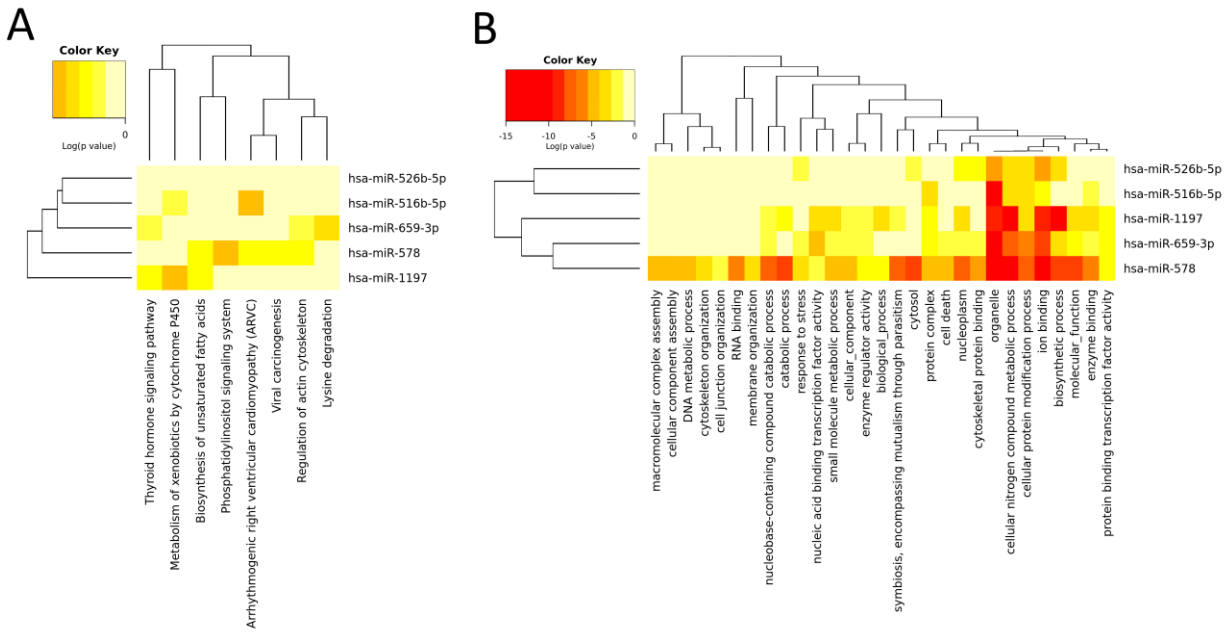

Supplemental Figure 2. KEGG and GOslim classifications of the circRNA-miRNA target genes. (A) KEGG and (B) GOslim categories union of the RNA targets of the five miRNAs sequestered by three or more of the deregulated PD circRNAs (miR-516b-5p, miR-526b-5p, miR-578, miR-659-3p, miR-1197). They were prepared using the DIANA-miRPath v3.0 interface using default values (p-value threshold 0.05, microT-CDS threshold 0.8).

TABLES

Table 1. Demographic and clinical profiles of healthy controls and PD patients.

Variables	**Healthy controls**	**iPD**	***P* value**
No of subjects	60	60	N/A
Age [a]	64.38 ± 1.335	64.73 ± 1.33	0.84
Sex (M/F)	29/31	29/31	1
Age of onset [a]	N/A	59.95 ± 10.97	N/A
Disease duration [a, b]	N/A	4.78 ± 0.55	N/A
UPDRS III [a, c] **(on/off state)**	N/A	25.77 ± 1.92 (42/18)	N/A
MMSE [a, d]	N/A	27.53 ± 0.56	N/A
H&Y [a, e]	N/A	1.82 ± 0.10	N/A
LEDD [a, f]	N/A	496.9 ± 59.71	N/A

[a] ± SD.

[b] Disease duration is counted in years.

[c] Unified Parkinson's Disease Rating Scale.

[d] Mini Mental State Examination.

[e] Hoehn & Yahr.

[f] Levodopa equivalent daily dose.

SUPPLEMENTAL TABLES

Supplemental Table 1. Primer sequences used for real-time PCR.

circRNA	Forward	Reverse
hsa_AFF2_circ_0001947	ACTGCCAAAGTTCACCATCC	AGTTTCCAAGCGTGTTCTGG
hsa_AGTPBP1_circ_0007162	GTGGATTCGTATGGGGACTG	CCTGCCGTAGGAACAACAAT
hsa_ANKRD12_circ_0000826	CGTCCAGTGGATGTAGCAGA	AACCCAGATTTGGGCATTTT
hsa_ANKS1B_circ_0007294	TGGGAAAAATGGAAGCCAGAGT	AGAACTCGTACAACATCCACCT
hsa_ARPP21_circ_0001281	GTCCATCGAGTGGCAGCTT	ATGCCCATCTCCATGCGATT
hsa_ATP6V0A1 _circ_0043837	CGCCGTCAGTATTTGAGGAG	GGCTGACTCCAAACAGCATA
hsa_BACH1_circ_0001181	CGCTGTCGCAAGAGAAAAC	AGGCAAAAACCGAGTTCTCA
hsa_CDR1_circ_0001946	CATGTCTTCCAACGTCTCCA	ACCTTGACACAGGTGCCATC
hsa_CNTNAP2_circ_0133631	GGATGCTCTACAGCGACACA	GGGAGTCCAGAGACAAGTGG
hsa_CORO1C_circ_0000437	ATGGGTTACATGCCCAAGAG	ACACCCCATTGCTAGTGTCC
hsa_CSNK1G3_circ_0001522	GCACCACAGCTACATTTGGA	GCATGTTCATCCCATTCGT
hsa_DAB1_circ_0113684	TGTGCCAAAAAGTCAACCTG	CCCGGTGATCTGTAATGTCC
hsa_DGKB_circ_0133622	AGGAGACCCAGTGCCTTACA	GGTCCTTCAAAGGTCCACAG
hsa_DNAJC6_circ_0002454	TGACATTCGAAGCTTTTTGG	ATAGCTGGGCTCCATGTCTG
hsa_ DOP1B_circ_0001187	GGAATGTTCTCAGAAAGGAGGA	AATGTTTTCCCTCTTGGAGGT
hsa_ERC2_circ_0124264	CGGATTGAGAGGAGGAAACA	TTGATTGTGCTTGAGGTTGG
hsa_EXOC6B_circ_0009043	TCCGCAAACATTCAGACAAA	GCTTCAGCTCTTCCATTGCT
hsa_EXOSC1_circ_0005887	CCCGAATTCTTGCAGACCTA	ACCTGGGCGGAAACTCTTAT
hsa_FAM120A_circ_0001875	TGTCATTTCATCCACCACATT	CAAGCCATGGAAACCATTCT
hsa_FGD4_circ_0000390	TAGCTGCTCGGAACACTTCA	GCATGTGATGCTGCAAAGTT
hsa_FKBP3_circ_0101874	AAGGCTCGACTGGAGATTGA	GCTGTCTTGGCCACATTTTT
hsa_FUT8_circ_0003028	GTCCAAGATTCTGGCAAAGC	TCAAAGAGATCCTCCTGGTGA
hsa_GBAS_circ_0001709	GAATGAGCCTGTGCCAAGAT	TTCTGTGAGGGCTGGATAGC

hsa_GRIN2B_circ_0097968	CTGAGCCCAAAAGCAGTTGT	TTACGGAAGCTTGCTGTTCA
hsa_HAGH_circ_0105101	CAGGGAGAAGGACCAGTTCA	GCTCCCCGATGCTGTACTT
hsa_HAT1_circ_0008032	TGCTGGTAGCCTGTCAACAA	GCCAGTTTCTTCTCCACTGC
hsa_HIPK3_circ_0000284	TCGGCCAGTCATGTATCAAA	GGGTAGACCAAGACTTGTGAGG
hsa_HMGCLL1_circ_0131944	CAGGTGCTCTTGCTGTTCAC	CATCCCTAGGCCCAACTTCT
hsa_HOMER1_circ_0006916	AATGCATTGCCATTTTCACA	TGTGTTTGGGTCAATTTGGA
hsa_HTT_circ_0001392	TTTGGCAATTTTGCAAATGA	CACACGGTCTTTCTTGGTAGC
hsa_KCNN2_circ_0127664	CCGAGCTTGTGAAAGTTGTTC	CACACACCAGTATTTCCAAGCA
hsa_KDM4C_circ_0001839	ATGGCTACCATGCTGGTTTT	TCAAGTCGTTTTCCATGCTC
hsa_KIAA1841_circ_0007793	GGACCGAGTCAAGTCAAAGG	TGGGCACAGGGTGAAGATAC
hsa_KIDINS220_circ_0005315	ACCGGACTTCATGGCTCATA	CCTCTGCATCTGCCTTCTTC
hsa_KLHL1_circ_0100796	GGAATTCGAGCCTTCGCAGA	TGGAGTCCAAATCACTTTGAGGT
hsa_LMBR1_circ_0005939	GGCTAAATGGCTCCCTGATT	CGATGGCATCTTCATCTTCTT
hsa_LPAR1_circ_0087960	GGCTGCCATCTCTACTTCCA	GTGGATGGGGAGCTTCATAA
hsa_LRCH1_circ_0002215	GGAAGCATGCCGAAAATTAG	TCCTCCGGATTGTAAACTGC
hsa_LRCH3_circ_0002266	TCCCAAATTGGTAACCTGGA	CCAGAGAAACAAAGTGACATGCT
hsa_LRRC7_circ_0114013	TGGACAAGGAAATCCATTCA	TCCATTGGCCACTAGGAGAT
hsa_MAPK8_circ_0002968	TGTGGAATCAAGCACCTTCA	AAAAATTGTTGTCACGCTTGC
hsa_MAPK9_circ_0001566	TGGAGCTGGATCATGAAAGA	AAGGGTGGGCAAGTTTCAG
hsa_MED12L_circ_0067735	CAACGTGGCTGATCAAGATG	GGCTGGCTGATTATTGAAGC
hsa_NRXN1_circ_0054525	TTCCAGGGTCACCAGTCAGT	GATCCTTTGAACGTGGCAAT
hsa_NTRK2_circ_0139142	CCTGAATGAAAGCAGCAAGA	ACCTTTTCTGGTTTGCGATG
hsa_PAK3_circ_0139566	GTTGGGGACCCAAAGAAAAA	ATCAAACCCCACATGAATCG
hsa_PDE4B_circ_0008433	ACTGCCTTTGACAACGCTTC	TTCAATGCAGTTTGCTGACA
hsa_PHC3_circ_0001359	TGTCACCCGGACATCAAGTA	GGGTAATACTGCCGCTGGTA
hsa_POMT1_circ_0001897	CTGGCCTTGGGAGGTTATTT	GCCCACTGTCATCCAAGAAG
hsa_PPP2R2B_circ_0128256	GCGTGATAAGAGGCCAGAAG	AATTCTCCCGTGTGGTTGAA

hsa_PRKCB_circ_0000682	ACAGGGACGTCCTCATTGTC	GTCACATTTCATCCCCTGGT
hsa_PSD3_circ_0002111	TGCAAGGGGTAAATGAGGGTG	TTCAGTGCTCCCCATTTCAGA
hsa_PSEN1_circ_0003848	AGTTACCTGCACCGTTGTCC	GCTGTCTAAGGACCGCAAAG
hsa_PTK2_circ_0003171	GATGGCTCCAGAGTCAATCAA	CTCACGCTGTCCGAAGTACA
hsa_R3HDM1_circ_0001070	AAGGATCTATGCCCACAACAGG	GACTCTGGGGTTGCTGAACT
hsa_REPS1_circ_0004368	CCATTCAGCCTGATCTAAACG	ACACTGCATCACCAGCAGAA
hsa_RERE_circ_0002158	TAAAGCCCGAGTGGATTCAT	TGACGTTCATGAGGAGATGG
hsa_RIMS1_circ_0132246	GGAGATCCAGCCTTAGTGCC	AGCTTGCTTTTGTGGAAGAGT
hsa_RIMS1_ circ_0132250	AGCAGGTGGAAAGAAACGGA	TGTCTTGTTCGCTCCTCCAC
hsa_RIMS2_circ_0005114	TCTGTCACGGAAAAGTCGCA	TGATCCGGCTACCTGTTTGT
hsa_RMST_circ_0099634	AGGGGCTAGTTGAGGAATGG	CCATTCTGTGCTGAGTGGAG
hsa_RTN4_circ_0054598	GAGGACAGATCACCATCTGCTA	TGCAGAGGAGCGTATCACAG
hsa_SCAF8_circ_0001654	CTTGCGGCTGTAGCTCAGAT	TTTGGGTCATTTTCGCTTTC
hsa_SCLT1_circ_0001439	GAACATGGAAGTGACTAACCAACA	GGGAAAGGCCTCCAATTTT
hsa_SFMBT2_circ_0000211	ATGGCCTCTGAATGGAAATG	CTCGAACCAGTCAAGTCACG
hsa_SLAIN1_circ_0000497	GCTTGCATGGAGCTGGAAATG	ATGTCTACACCACTGCAAAGGA
hsa_SLAIN2_circ_0126525	AAGTGCCAAACGGAGGAATA	AATCCAAAACTTGCCTGCAC
hsa_SLC30A6_circ_0005695	CCGTGCCTGAGCAATAGTTT	TGCACCACATAAGCAGGAAG
hsa_SLC38A1_circ_0000396	CATTATGGGCAGTGGGATTT	GTATGGCCTTCCAGGGTTTT
hsa_SMARCA5_circ_0001445	TGGGCGAAAGTTCACTTAGAA	GAAGCATTTCATCTTTCCCAAT
hsa_STX6_circ_0007905	GGCTGGACAATGTGATGAAG	GCCTGCACAGATGAAGTTGA
hsa_SYT1_circ_0099287	ACAGTGGATTTTGGCCATGT	AAAAGCAGCAGGTCAGGACT
hsa_TMCC1_circ_0001340	GGGAAGCTATTGCTGGGATT	ACCAAAGGCAACTGTTCACC
hsa_TMEFF1_circ_0004425	GGTCAGGGGCAGAAGTTCAC	CTCTTACGTCAGACTCCCTCAC
hsa_TMEM132D_circ_0097876	CAAAGACCGTGAGGAAAGGA	GCAAGGAAAACCTCTGGATG
hsa_TMEM138_circ_0002058	GCTGGAAAAACTCCAACAGC	AGCCTGGAAGACGAAGGTGT
hsa_UBE2K_circ_0002590	CAGAGCCAGATGATCCACAG	GTGTGTCTGGAGGTCCTGCT

hsa_UBXN7_circ_0001380	TGCATAAAGGCAGCTTTGAA	CCGTCGTCTTTTAGGAGCAC
hsa_UIMC1_circ_0001558	CCCACAAAGATTGAACGACA	GCAGCAACACTTTGTGAAGC
hsa_UNC13C_circ_0103896	AAAGCAAATGGCAGAGTTGG	AAACCAGAAGCAAAGCTCCA
hsa_VMP1_circ_0006508	TCTTCTGTTGGGCTTGGAAC	TTCCATTCTCTGCCATTTCA
hsa_VPS13C_circ_0000607	AAGCACAGGCAGTTACTCAAGA	GCATGGAGTCCAGTGTTCATT
hsa_WDR78_circ_0006677	GAAGACCTGGAAGAACCATCC	TCTGCTTTGATTTGCACCAG
hsa_YY1AP1_circ_0014606	ATTCTGGACCCAGCACAAAG	TCTTCTGGGCCATCATCTTC
hsa_ZFAND6_circ_0000643	TGTGGACAAAGCAGTACCTGA	CCATTTGTACGAGGGTTTCC
hsa_ZMYM4_circ_0011536	GCACCACAGCAGGGACTACT	ATCCTGTTTGATTCGGCATT
hsa_ZNF292_circ_0004058	TTCTTTCCCAGGAACCATTG	CGGGCTTTAACATAACTTTGG
hsa-GAPDH	GCACCACCAACTGCTTAG	GCCATCCACAGTCTTCTG
hsa-U6	CGCTTCGGCAGCACATATAC	TTCACGAATTTGCGTGTCAT

Supplemental Table 2. List of 39 circRNAs not detected in PBMCs

ANKS1B_circ_0007294	KLHL1_circ_0100796	RERE_circ_0002158
ARPP21_circ_0001281	LMBR1_circ_0005939	RIMS1_circ_0132246
CDR1_circ_0001946	LPAR1_circ_0087960	RIMS1_circ_0132250
CNTNAP2_circ_0133631	LRCH1_circ_0002215	RIMS2_circ_0005114
DAB1_circ_0113684	LRRC7_circ_0114013	RMST_circ_0099634
DGKB_circ_0133622	NRXN1_circ_0054525	SCAF8_circ_0001654
ERC2_circ_0124264	NTRK2_circ_0139142	SLC30A6_circ_0005695
EXOSC1_circ_0005887	PAK3_circ_0139566	STX6_circ_0007905
FGD4_circ_0000390	PDE4B_circ_0008433	SYT1_circ_0099287
GRIN2B_circ_0097968	PPP2R2B_circ_0128256	TMEFF1_circ_0004425
HAGH_circ_0105101	PRKCB_circ_0000682	TMEM132D_circ_0097876
HMGCLL1_circ_0131944	PSD3_circ_0002111	UNC13C_circ_0103896
KCNN2_circ_0127664	PTK2_circ_0003171	YY1AP1_circ_0014606

Supplemental Table 3. Basic characteristics and comparative PBMC circRNA expression in idiopathic PD patients and healthy controls.

CircRNA size and expression in the brain as well as host transcript expression in the body. Means with their respective standard deviation (std) for both groups are shown. Statistically significant differences in comparison to healthy controls (unpaired t-test) are highlighted in grey. Multiple comparison analysis (adjusted *P* values) calculated according to Benjamini-Hochberg false discovery rate method.

circRNA ID	Spliced Seq length	Expression score in the human brain*	Host gene symbol	Host gene mRNA expression in the human body**	Mean (± std)		Unpaired t-test *P* value	Adjusted *P* values
					HC	iPD		
circ_0001380	247	15326	UBXN7	Ubiquitous, expressed least in the brain except cerebellum where expression is similar to other tissues	-0.046 (0.348)	-0.016 (0.432)	0.678	0.812
circ_0000284	1099	13889	HIPK3	Ubiquitous, expressed least in the brain	-0.073 (0.443)	-0.165 (0.435)	0.252	0.603
circ_0001445	269	9354	SMARCA5	Ubiquitous, lower expression in the brain	-0.132 (0.565)	-0.275 (0.504)	0.147	0.415
circ_0009043	390	9121	EXOC6B	Ubiquitous, enriched in the skin	-0.061 (0.395)	-0.089 (0.425)	0.701	0.812
circ_0001947	861	9058	AFF2	Ubiquitous, highly enriched in the cerebellum	-0.208 (0.702)	-0.302 (0.531)	0.412	0.706
circ_0002590	336	8841	UBE2K	Ubiquitous, enriched in the cerebellum	-0.062 (0.409)	-0.073 (0.437)	0.895	0.895
circ_0000437	251	8402	CORO1C	Ubiquitous, expressed least in the brain	-0.224 (0.736)	0.007 (0.911)	0.130	0.390
circ_0000497	788	6004	SLAIN1	Brain-specific	-0.096 (0.520)	-0.447 (0.313)	<0.0001 ***	0.001***
circ_0054598	2457	5985	RTN4	Ubiquitous, enriched in the brain	-0.165 (0.624)	-0.139 (0.583)	0.815	0.850
circ_0001522	536	5649	CSNK1G3	Ubiquitous, lower expression in the brain	-0.077 (0.452)	-0.190 (0.505)	0.205	0.518
circ_0001070	307	5300	R3HDM1	Brain-specific	-0.058 (0.394)	0.050 (0.523)	0.204	0.518
circ_0011536	755	4662	ZMYM4	Ubiquitous, expressed least in the brain except	-0.064 (0.417)	-0.093 (0.406)	0.694	0.812

				cerebellum where expression is somewhat higher than in other tissues				
circ_0000607	606	4056	VPS13C	Ubiquitous, expressed least in the brain except cerebellum where expression is similar to other tissues	-0.078 (0.449)	0.021 (0.514)	0.266	0.603
circ_0001439	396	3870	SCLT1	Ubiquitous, expressed least in the brain except cerebellum where expression is somewhat higher than in other tissues	-0.056 (0.399)	-0.209 (0.429)	0.046*	0.210
circ_0000826	994	3868	ANKRD12	Ubiquitous, expressed least in the brain except cerebellum where expression is somewhat higher than in other tissues	-0.059 (0.405)	-0.217 (0.355)	0.024*	0.142
circ_0000211	434	3783	SFMBT2	Ubiquitous	-0.076 (0.457)	-0.239 (0.381)	0.036*	0.189
circ_0002266	378	3204	LRCH3	Ubiquitous, expressed least in the brain except cerebellum where expression is somewhat higher than in other tissues	-0.089 (0.458)	-0.045 (0.433)	0.595	0.782
circ_0002968	499	3123	MAPK8	Ubiquitous, highly enriched in the cerebellum	-0.047 (0.361)	-0.087 (0.476)	0.603	0.782
circ_0000396	522	3086	SLC38A1	Ubiquitous	-0.097 (0.498)	-0.237 (0.472)	0.115	0.380
circ_0001181	1836	3082	BACH1	ubiquitous, expressed least in the brain	-0.203 (0.691)	-0.399 (0.538)	0.086	0.344
circ_0006916	522	3026	HOMER1	Ubiquitous, enriched in the brain	-0.076 (0.452)	-0.292 (0.316)	0.003**	0.036*
circ_0001709	212	2889	GBAS	Ubiquitous, highly enriched in the skeletal muscle	-0.047 (0.354)	-0.060 (0.359)	0.839	0.857
circ_0001897	158	2882	POMT1	Ubiquitous, highly enriched in the cerebellum and testis	-0.069 (0.426)	-0.139 (0.439)	0.375	0.667
circ_0101874	502	2687	FKBP3	Ubiquitous, enriched in the brain	-0.059 (0.395)	-0.136 (0.482)	0.347	0.640
circ_0002454	350	2511	DNAJC6	Brain-specific	-0.247 (0.728)	-0.027 (0.806)	0.119	0.380
circ_0001558	397	2476	UIMC1	Ubiquitous, expressed least in the brain except cerebellum where expression is similar to other tissues	-0.095 (0.498)	0.028 (0.497)	0.459	0.711

circ_0001187	301	2263	DOP1B	Ubiquitous, highly enriched in the cerebellum	-0.071 (0.440)	-0.265 (0.282)	0.005**	0.038*
circ_0006508	440	2229	VMP1	Ubiquitous, expressed least in the brain	-0.058 (0.384)	-0.031 (0.402)	0.711	0.812
circ_0006677	473	2190	WDR78	Testis, lung	-0.072 (0.439)	-0.051 (0.492)	0.801	0.850
circ_0008032	302	2153	HAT1	Ubiquitous, expressed least in the brain	-0.133 (0.579)	-0.204 (0.526)	0.482	0.723
circ_0043837	444	1892	ATP6V0A1	Ubiquitous, highly enriched in the brain	-0.142 (0.611)	-0.250 (0.597)	0.334	0.640
circ_0004368	352	1882	REPS1	Ubiquitous, highly enriched in the cerebellum	-0.076 (0.455)	-0.299 (0.313)	0.002**	0.036*
circ_0005315	308	1820	KIDINS220	Ubiquitous, enriched in the cerebellum	-0.149 (0.554)	-0.194 (0.438)	0.628	0.793
circ_0002058	248	1775	TMEM138	ubiquitous, expressed least in the brain	-0.055 (0.379)	0.028 (0.465)	0.286	0.603
circ_0001566	497	1745	MAPK9	Ubiquitous, enriched in the brain	-0.066 (0.425)	-0.284 (0.352)	0.002**	0.036*
circ_0007793	284	1645	KIAA1841	Ubiquitous, somewhat brain-enriched	-0.141 (0.591)	-0.168 (0.556)	0.793	0.850
circ_0001340	251	1631	TMCC1	Ubiquitous, enriched in the cerebellum	-0.054 (0.380)	-0.108 (0.389)	0.443	0.711
circ_0007162	1121	1526	AGTPBP1	Ubiquitous, somewhat brain-enriched	-0.103 (0.524)	-0.317 (0.434)	0.017*	0.113
circ_0003848	222	1430	PSEN1	Ubiquitous, highly enriched in the spinal cord	-0.054 (0.388)	-0.241 (0.308)	0.004**	0.038*
circ_0004058	370	1422	ZNF292	Ubiquitous, expressed least in the brain except cerebellum where expression is similar to other tissues	-0.095 (0.491)	-0.045 (0.479)	0.577	0.782
circ_0001875	556	1345	FAM120A	Ubiquitous, expressed least in the brain	-0.098 (0.504)	-0.196 (0.500)	0.289	0.603
circ_0003028	430	1336	FUT8	Ubiquitous, highly enriched in the spinal cord	-0.270 (0.792)	-0.309 (0.654)	0.850	0.850
circ_0001839	292	1280	KDM4C	Ubiquitous, highly enriched in the cerebellum	-0.066 (0.418)	-0.115 (0.482)	0.557	0.782
circ_0001392	484	1270	HTT	Ubiquitous, enriched in the cerebellum	-0.060 (0.384)	-0.019 (0.453)	0.602	0.782
circ_0067735	457	952	MED12L	Adrenal glands, brain, cervix, pituitary and testis	-0.477 (1.100)	-0.124 (1.202)	0.096	0.354
circ_0000643	381	761	ZFAND6	Ubiquitous, expressed least in the brain	-0.090 (0.477)	-0.173 (0.467)	0.341	0.640
circ_0126525	971	720	SLAIN2	Ubiquitous, expressed least in the brain	-0.075 (0.450)	0.125 (0.628)	0.048*	0.210
circ_0001359	505	709	PHC3	Ubiquitous, expressed least in the brain	-0.060 (0.403)	-0.118 (0.434)	0.454	0.711

*According to Rybak et al.

** According to GTEx portal.

Supplemental Table 4. Correlation between relative circRNA expression and sex, age, age-at-onset, PD duration, HY, UPDRS and MMSE scores and LEDD of PD patients.

circRNA	Sex U score (*P* value)	Age Rho (*P* value)	Age-at-onset Rho (*P* value)	PD duration Rho (*P* value)	UPDRS III Rho (*P* value)	MMSE Rho (*P* value)	HY Rho (*P* value)	LEDD Rho (*P* value)
UBXN7_circ_0001380	0.027 (0.8684)	-0.012 (0.8949)	-0.142 (0.2831)	0.041 (0.7579)	0.143 (0.2788)	0.096 (0.4674)	0.113 (0.3953)	0.055 (0.6791)
HIPK3_circ_0000284	1.694 (0.1930)	0.004 (0.9627)	-0.129 (0.3266)	-0.063 (0.6303)	-0.036 (0.7847)	0.090 (0.4924)	-0.052 (0.6943)	0.100 (0.4450)
SMARCA5_circ_0001445	0.778 (0.3776)	-0.035 (0.7078)	-0.119 (0.3663)	-0.174 (0.1847)	0.018 (0.8931)	0.082 (0.5321)	0.005 (0.9704)	0.006 (0.9643)
EXO6CB_circ_0009043	1.129 (0.2880)	0.142 (0.1215)	0.225 (0.0836)	-0.116 (0.3793)	-0.014 (0.9165)	-0.021 (0.8736)	-0.066 (0.6187)	-0.024 (0.8551)
AFF2_circ_0001947	0.011 (0.9159)	0.107 (0.2446)	0.101 (0.4418)	-0.036 (0.7871)	0.050 (0.7055)	-0.048 (0.7130)	-0.138 (0.2917)	0.156 (0.2334)
UBE2K_circ_0002590	0.010 (0.9208)	-0.035 (0.7022)	-0.143 (0.2773)	-0.187 (0.1535)	-0.167 (0.2024)	0.065 (0.6205)	-0.012 (0.9295)	-0.139 (0.2898)
CORO1C_circ_0000437	0.035 (0.8521)	-0.089 (0.3313)	-0.390 (0.0021)	0.211 (0.1050)	0.090 (0.4928)	0.039 (0.7691)	0.019 (0.8856)	0.183 (0.1618)
SLAIN1_circ_0000497	0.026 (0.8717)	-0.098 (0.2870)	-0.085 (0.5188)	-0.109 (0.4071)	0.094 (0.4771)	0.257 (0.0472)	0.132 (0.3146)	0.050 (0.7061)
RTN4_circ_0054598	3.005 (0.0830)	0.035 (0.7015)	-0.203 (0.1191)	-0.073 (0.5807)	-0.033 (0.8049)	0.077 (0.5578)	-0.016 (0.9048)	0.027 (0.8353)
CSNK1G3_circ_0001522	3.347 (0.0673)	-0.049 (0.5978)	0.083 (0.5300)	-0.217 (0.0987)	-0.018 (0.8931)	0.172 (0.1924)	-0.088 (0.5066)	-0.115 (0.3837)
R3HDM1_circ_0001070	0.078 (0.7798)	0.010 (0.9160)	0.033 (0.8001)	-0.127 (0.3322)	-0.224 (0.0850)	0.061 (0.6445)	-0.156 (0.2326)	-0.153 (0.2434)
ZMYM4_circ_0011536	3.556 (0.0593)	-0.085 (0.3584)	-0.044 (0.7413)	-0.341 (0.0078)	-0.123 (0.3479)	0.122 (0.3540)	0.000 (0.9976)	-0.081 (0.5403)

VPS13C_circ_0000607	0.001 (0.9802)	0.049 (0.5951)	0.018 (0.8923)	-0.048 (0.7134)	-0.073 (0.5790)	-0.204 (0.1181)	0.090 (0.4930)	-0.058 (0.6610)
SCLT1_circ_0001439	0.028 (0.8668)	0.016 (0.8636)	-0.159 (0.2264)	-0.037 (0.7774)	0.094 (0.4769)	0.048 (0.7169)	0.055 (0.6761)	0.184 (0.1589)
ANKRD12_circ_0000826	0.285 (0.5931)	0.008 (0.9346)	-0.091 (0.4876)	0.016 (0.9014)	0.090 (0.4944)	-0.023 (0.8612)	0.165 (0.2071)	0.116 (0.3755)
SFMBT2_circ_0000211	0.519 (0.4711)	0.100 (0.2778)	0.008 (0.9543)	-0.114 (0.3873)	0.053 (0.6898)	0.244 (0.0598)	0.092 (0.4864)	0.003 (0.9828)
LRCH3_circ_0002266	0.556 (0.4559)	-0.042 (0.6471)	-0.094 (0.4739)	-0.236 (0.0692)	-0.104 (0.4283)	0.087 (0.5074)	0.070 (0.5965)	-0.061 (0.6453)
MAPK8_circ_0002968	0.846 (0.3578)	-0.064 (0.4898)	0.037 (0.7785)	-0.163 (0.2146)	0.040 (0.7634)	0.096 (0.4648)	0.115 (0.3814)	-0.090 (0.4943)
SLC38A1_circ_0000396	0.062 (0.8037)	-0.111 (0.2284)	0.207 (0.1124)	-0.149 (0.2565)	0.024 (0.8558)	0.087 (0.5068)	0.004 (0.9766)	-0.135 (0.3040)
BACH1_circ_0001181	3.978 (0.0461)	-0.133 (0.1488)	-0.110 (0.4034)	-0.028 (0.8333)	0.070 (0.5948)	0.070 (0.5932)	0.066 (0.6146)	0.254 (0.0498)
HOMER1_circ_0006916	0.102 (0.7490)	-0.112 (0.2253)	-0.040 (0.7623)	-0.090 (0.4928)	0.099 (0.4499)	0.068 (0.6068)	0.157 (0.2318)	0.032 (0.8105)
GBAS_circ_0001709	0.892 (0.3450)	-0.041 (0.6604)	-0.066 (0.6138)	-0.001 (0.9951)	0.111 (0.4003)	0.201 (0.1244)	0.185 (0.1566)	0.025 (0.8487)
POMT1_circ_0001897	1.293 (0.2555)	0.032 (0.7285)	0.002 (0.9851)	-0.130 (0.3239)	-0.006 (0.9630)	-0.095 (0.4723)	0.012 (0.9301)	-0.011 (0.9336)
FKBP3_circ_0101874	0.030 (0.8633)	-0.073 (0.4314)	-0.009 (0.9472)	-0.142 (0.2839)	0.104 (0.4318)	0.111 (0.4040)	0.016 (0.9041)	0.050 (0.7091)
DNAJC6_circ_0002454	0.575 (0.4485)	-0.107 (0.2443)	-0.379 (0.0028)	0.000 (0.9985)	-0.011 (0.9352)	0.019 (0.8864)	-0.008 (0.9514)	0.078 (0.5516)
U1MC1_circ_0001558	2.384 (0.1226)	-0.010 (0.9113)	-0.070 (0.5960)	-0.223 (0.0868)	-0.181 (0.1657)	0.083 (0.5273)	-0.104 (0.4310)	-0.035 (0.7909)
DOP1B_circ_0001187	0.812 (0.3676)	-0.035 (0.7063)	0.020 (0.8778)	-0.101 (0.4416)	-0.147 (0.2623)	-0.075 (0.5711)	-0.156 (0.2354)	-0.267 (0.0396)
VMP1_circ_0006508	0.785 (0.3756)	-0.071 (0.4460)	-0.188 (0.1534)	-0.123 (0.3538)	-0.053 (0.6923)	0.166 (0.2081)	0.046 (0.7298)	-0.112 (0.3980)
WDR78_circ_0006677	0.547 (0.4596)	-0.086 (0.3541)	-0.252 (0.0545)	-0.074 (0.5794)	-0.037 (0.7812)	0.071 (0.5919)	0.044 (0.7407)	0.001 (0.9918)
HAT1_circ_0008032	4.783 (0.0287)	-0.039 (0.6710)	-0.098 (0.4550)	-0.131 (0.3176)	0.018 (0.8914)	0.100 (0.4488)	0.138 (0.2922)	0.030 (0.8196)

ATP6V0A1_ circ_0043837	0.010 (0.9208)	0.048 (0.6025)	-0.111 (0.3978)	0.095 (0.4719)	-0.001 (0.9958)	-0.008 (0.9523)	-0.072 (0.5843)	0.070 (0.5971)
REPS1_circ _0004368	0.363 (0.5467)	0.012 (0.8933)	0.108 (0.4099)	-0.206 (0.1135)	-0.009 (0.9453)	-0.148 (0.2587)	-0.023 (0.8642)	-0.054 (0.6831)
KIDINS220_ circ_0005315	4.019 (0.0450)	0.010 (0.9103)	-0.093 (0.4845)	-0.076 (0.5681)	0.058 (0.6643)	0.227 (0.0833)	0.036 (0.7864)	0.020 (0.8785)
TMEM138_ circ_0002058	0.020 (0.8864)	0.032 (0.7304)	-0.008 (0.9521)	-0.030 (0.8227)	0.014 (0.9144)	-0.043 (0.7471)	0.068 (0.6034)	0.030 (0.8221)
MAPK9_circ _0001566	1.954 (0.1621)	0.044 (0.6357)	-0.119 (0.3663)	0.063 (0.6301)	0.062 (0.6389)	0.202 (0.1208)	0.057 (0.6662)	-0.010 (0.9406)
KIAA1841_ circ_0007793	0.034 (0.8546)	-0.014 (0.8824)	-0.179 (0.1715)	-0.027 (0.8372)	0.089 (0.4983)	0.025 (0.8473)	0.050 (0.7058)	0.244 (0.0601)
TMCC1_circ _0001340	0.053 (0.8185)	-0.006 (0.9453)	-0.104 (0.4335)	-0.049 (0.7133)	0.026 (0.8473)	0.093 (0.4816)	0.045 (0.7331)	0.049 (0.7141)
AGTPBP1_ circ_0007162	0.068 (0.7941)	0.033 (0.7198)	-0.047 (0.7215)	-0.076 (0.5616)	0.168 (0.1995)	0.156 (0.2330)	0.110 (0.4023)	0.264 (0.0413)
PSEN1_circ _0003848	0.148 (0.7001)	0.002 (0.9865)	-0.263 (0.0424)	0.012 (0.9249)	0.077 (0.5594)	0.160 (0.2218)	0.010 (0.9394)	0.244 (0.0606)
ZNF292_circ _0004058	0.121 (0.7283)	-0.020 (0.8305)	-0.089 (0.5008)	-0.232 (0.0770)	-0.022 (0.8662)	0.077 (0.5620)	-0.038 (0.7733)	-0.074 (0.5774)
FAM120A_ circ_0001875	0.047 (0.8279)	-0.082 (0.3747)	-0.237 (0.0687)	-0.145 (0.2675)	-0.070 (0.5942)	0.129 (0.3253)	-0.041 (0.7551)	-0.009 (0.9473)
FUT8_circ _0003028	0.493 (0.4826)	-0.074 (0.4238)	-0.214 (0.1004)	0.029 (0.8233)	-0.040 (0.7600)	0.072 (0.5852)	-0.094 (0.4761)	-0.114 (0.3875)
KDM4C_circ _0001839	0.030 (0.8619)	0.070 (0.4462)	0.122 (0.3525)	-0.183 (0.1627)	-0.177 (0.1753)	0.069 (0.6028)	-0.153 (0.2436)	-0.121 (0.3555)
HTT_circ _0001392	1.317 (0.2512)	-0.092 (0.3232)	-0.045 (0.7327)	-0.101 (0.4470)	0.078 (0.5564)	0.118 (0.3754)	0.054 (0.6859)	-0.006 (0.9664)
MED12L_circ _0067735	1.103 (0.2937)	-0.137 (0.1368)	-0.415 (0.0010)	0.221 (0.0893)	0.066 (0.6178)	0.050 (0.7037)	0.008 (0.9512)	0.246 (0.0580)
ZFAND6_circ _0000643	4.280 (0.0386)	-0.053 (0.5659)	-0.138 (0.2939)	-0.148 (0.2585)	-0.046 (0.7246)	0.098 (0.4573)	-0.029 (0.8284)	-0.108 (0.4101)
SLAIN2_circ _0126525	0.623 (0.4301)	0.015 (0.8669)	-0.060 (0.6462)	-0.135 (0.3030)	-0.100 (0.4489)	0.096 (0.4651)	-0.043 (0.7458)	-0.039 (0.7653)
PHC3_circ _0001359	0.418 (0.5182)	-0.003 (0.9738)	-0.064 (0.6282)	-0.217 (0.0951)	-0.068 (0.6062)	0.139 (0.2897)	-0.037 (0.7778)	-0.077 (0.5598)

Significance Supplemental Table 5. KEGG and GOslim categories that are mostly deregulated in idiopathic PD. Gene union of the targets of the five miRNAs (miR-516b-5p, miR-526b-5p, miR-578, miR-659-3p, miR-1197) sequestered by half or more of the deregulated PD circRNAs in PD versus (A) KEGG and (B) GOslim categories created by the DIANA-miRPath v3.0 interface using default values (*p*-value threshold 0.05, microT-CDS threshold 0.8).

A

KEGG pathway	*P* value	# genes	# miRNAs
Thyroid hormone signaling pathway	0.001458	24	5
Cell cycle	0.009263	25	5
Regulation of actin cytoskeleton	0.014546	42	5
Rap1 signaling pathway	0.01546	35	5
Phosphatidylinositol signaling system	0.015883	16	4
MAPK signaling pathway	0.015883	46	5
FoxO signaling pathway	0.015883	26	5

B

GOslim category	*P* value	# genes	# miRNAs
Organelle	1.13E-78	1143	5
Cellular nitrogen compound metabolic process	6.05E-47	587	5
Cellular protein modification process	3.93E-19	283	5
Nucleoplasm	2.34E-13	159	5
Enzyme binding	2.34E-13	168	5

Protein complex	4.38E-11	411	5
Protein binding transcription factor activity	6.74E-10	70	5
Cytoskeletal protein binding	3.91E-09	102	5
Cell death	7.91E-08	112	5
RNA binding	6.93E-07	207	5
Nucleic acid binding transcription factor activity	7.74E-07	112	5
Macromolecular complex assembly	3.06E-05	95	5
Response to stress	3.72E-05	225	5
Membrane organization	4.89E-05	65	5
Cytoskeleton organization	0.000178	80	5

REFERENCES

1. Postuma RB, Berg D, Stern M, et al. MDS clinical diagnostic criteria for Parkinson's disease. Movement disorders : official journal of the Movement Disorder Society 2015;30(12):1591-1601.

2. Bhidayasiri R, Martinez-Martin P. Clinical Assessments in Parkinson's Disease: Scales and Monitoring. International review of neurobiology 2017;132:129-182.

3. Miller DB, O'Callaghan JP. Biomarkers of Parkinson's disease: present and future. Metabolism: clinical and experimental 2015;64(3 Suppl 1):S40-46.

4. Memczak S, Jens M, Elefsinioti A, et al. Circular RNAs are a large class of animal RNAs with regulatory potency. Nature 2013;495(7441):333-338.

5. Salzman J, Gawad C, Wang PL, Lacayo N, Brown PO. Circular RNAs are the predominant transcript isoform from hundreds of human genes in diverse cell types. PloS one 2012;7(2):e30733.

512 6. Zaphiropoulos PG. Circular RNAs from transcripts of the rat cytochrome P450 2C24 gene:
513 correlation with exon skipping. Proceedings of the National Academy of Sciences of the United
514 States of America 1996;93(13):6536-6541.
515 7. Jeck WR, Sorrentino JA, Wang K, et al. Circular RNAs are abundant, conserved, and
516 associated with ALU repeats. Rna 2013;19(2):141-157.
517 8. Schwanhausser B, Busse D, Li N, et al. Global quantification of mammalian gene
518 expression control. Nature 2011;473(7347):337-342.
519 9. Abdelmohsen K, Panda AC, Munk R, et al. Identification of HuR target circular RNAs
520 uncovers suppression of PABPN1 translation by CircPABPN1. RNA biology 2017;14(3):361-369.
521 10. Hansen TB, Jensen TI, Clausen BH, et al. Natural RNA circles function as efficient
522 microRNA sponges. Nature 2013;495(7441):384-388.
523 11. Zimmerman AJ, Hafez AK, Amoah SK, et al. A psychiatric disease-related circular RNA
524 controls synaptic gene expression and cognition. Molecular psychiatry 2020.
525 12. Li Z, Huang C, Bao C, et al. Exon-intron circular RNAs regulate transcription in the
526 nucleus. Nature structural & molecular biology 2015;22(3):256-264.
527 13. Zhang Y, Zhang XO, Chen T, et al. Circular intronic long noncoding RNAs. Molecular
528 cell 2013;51(6):792-806.
529 14. Ashwal-Fluss R, Meyer M, Pamudurti NR, et al. circRNA biogenesis competes with pre-
530 mRNA splicing. Molecular cell 2014;56(1):55-66.
531 15. Koh W, Gonzalez V, Natarajan S, Carter R, Brown PO, Gawad C. Dynamic ASXL1 Exon
532 Skipping and Alternative Circular Splicing in Single Human Cells. PloS one
533 2016;11(10):e0164085.

534 16. You X, Vlatkovic I, Babic A, et al. Neural circular RNAs are derived from synaptic genes
535 and regulated by development and plasticity. Nature neuroscience 2015;18(4):603-610.
536 17. Mahmoudi E, Cairns MJ. Circular RNAs are temporospatially regulated throughout
537 development and ageing in the rat. Scientific reports 2019;9(1):2564.
538 18. Rybak-Wolf A, Stottmeister C, Glazar P, et al. Circular RNAs in the Mammalian Brain
539 Are Highly Abundant, Conserved, and Dynamically Expressed. Molecular cell 2015;58(5):870-
540 885.
541 19. Mehta SL, Dempsey RJ, Vemuganti R. Role of circular RNAs in brain development and
542 CNS diseases. Progress in neurobiology 2020;186:101746.
543 20. Lukiw WJ. Circular RNA (circRNA) in Alzheimer's disease (AD). Frontiers in genetics
544 2013;4:307.
545 21. Doxakis E. Post-transcriptional regulation of alpha-synuclein expression by mir-7 and mir-
546 153. The Journal of biological chemistry 2010;285(17):12726-12734.
547 22. Zhao Y, Alexandrov PN, Jaber V, Lukiw WJ. Deficiency in the Ubiquitin Conjugating
548 Enzyme UBE2A in Alzheimer's Disease (AD) is Linked to Deficits in a Natural Circular miRNA-
549 7 Sponge (circRNA; ciRS-7). Genes 2016;7(12).
550 23. Hanan M, Simchovitz A, Yayon N, et al. A Parkinson's disease CircRNAs Resource reveals
551 a link between circSLC8A1 and oxidative stress. EMBO molecular medicine 2020:e11942.
552 24. Paschou M, Doxakis E. Neurofibromin 1 Is a miRNA Target in Neurons. PloS one
553 2012;7(10):e46773.
554 25. Paschou M, Maier L, Papazafiri P, et al. Neuronal microRNAs modulate TREK two-pore
555 domain K(+) channel expression and current density. RNA biology 2020;17(5):651-662.

556 26. Tan CL, Plotkin JL, Veno MT, et al. MicroRNA-128 governs neuronal excitability and
557 motor behavior in mice. Science 2013;342(6163):1254-1258.
558 27. Zhang W, Kim PJ, Chen Z, et al. MiRNA-128 regulates the proliferation and neurogenesis
559 of neural precursors by targeting PCM1 in the developing cortex. eLife 2016;5.
560 28. Iturria-Medina Y, Khan AF, Adewale Q, Shirazi AH, Alzheimer's Disease Neuroimaging
561 I. Blood and brain gene expression trajectories mirror neuropathology and clinical deterioration in
562 neurodegeneration. Brain : a journal of neurology 2020;143(2):661-673.
563 29. Naughton BJ, Duncan FJ, Murrey DA, et al. Blood genome-wide transcriptional profiles
564 reflect broad molecular impairments and strong blood-brain links in Alzheimer's disease. Journal
565 of Alzheimer's disease : JAD 2015;43(1):93-108.
566 30. Pinho R, Guedes LC, Soreq L, et al. Gene Expression Differences in Peripheral Blood of
567 Parkinson's Disease Patients with Distinct Progression Profiles. PloS one 2016;11(6):e0157852.
568 31. Soreq L, Bergman H, Israel Z, Soreq H. Exon arrays reveal alternative splicing aberrations
569 in Parkinson's disease leukocytes. Neuro-degenerative diseases 2012;10(1-4):203-206.
570 32. van Heerden JH, Conesa A, Stein DJ, Montaner D, Russell V, Illing N. Parallel changes in
571 gene expression in peripheral blood mononuclear cells and the brain after maternal separation in
572 the mouse. BMC research notes 2009;2:195.
573 33. Soreq L, Salomonis N, Bronstein M, et al. Small RNA sequencing-microarray analyses in
574 Parkinson leukocytes reveal deep brain stimulation-induced splicing changes that classify brain
575 region transcriptomes. Frontiers in molecular neuroscience 2013;6:10.
576 34. Dubois B, Burn D, Goetz C, et al. Diagnostic procedures for Parkinson's disease dementia:
577 recommendations from the movement disorder society task force. Movement disorders : official
578 journal of the Movement Disorder Society 2007;22(16):2314-2324.

579 35. Tomlinson CL, Stowe R, Patel S, Rick C, Gray R, Clarke CE. Systematic review of
580 levodopa dose equivalency reporting in Parkinson's disease. Movement disorders : official journal
581 of the Movement Disorder Society 2010;25(15):2649-2653.
582 36. Maass PG, Glazar P, Memczak S, et al. A map of human circular RNAs in clinically
583 relevant tissues. Journal of molecular medicine 2017;95(11):1179-1189.
584 37. Dube U, Del-Aguila JL, Li Z, et al. An atlas of cortical circular RNA expression in
585 Alzheimer disease brains demonstrates clinical and pathological associations. Nature neuroscience
586 2019;22(11):1903-1912.
587 38. Gokool A, Anwar F, Voineagu I. The Landscape of Circular RNA Expression in the
588 Human Brain. Biological psychiatry 2020;87(3):294-304.
589 39. Dudekula DB, Panda AC, Grammatikakis I, De S, Abdelmohsen K, Gorospe M.
590 CircInteractome: A web tool for exploring circular RNAs and their interacting proteins and
591 microRNAs. RNA biology 2016;13(1):34-42.
592 40. Xia S, Feng J, Chen K, et al. CSCD: a database for cancer-specific circular RNAs. Nucleic
593 acids research 2018;46(D1):D925-D929.
594 41. Li JH, Liu S, Zhou H, Qu LH, Yang JH. starBase v2.0: decoding miRNA-ceRNA, miRNA-
595 ncRNA and protein-RNA interaction networks from large-scale CLIP-Seq data. Nucleic acids
596 research 2014;42(Database issue):D92-97.
597 42. Vlachos IS, Zagganas K, Paraskevopoulou MD, et al. DIANA-miRPath v3.0: deciphering
598 microRNA function with experimental support. Nucleic acids research 2015;43(W1):W460-466.
599 43. Ravanidis S, Bougea A, Papagiannakis N, et al. Circulating Brain-enriched MicroRNAs
600 for detection and discrimination of idiopathic and genetic Parkinson's disease. Movement disorders
601 : official journal of the Movement Disorder Society 2020;35(3):457-467.

602 44. Dzamko N, Zhou J, Huang Y, Halliday GM. Parkinson's disease-implicated kinases in the
603 brain; insights into disease pathogenesis. Frontiers in molecular neuroscience 2014;7:57.
604 45. Waetzig V, Zhao Y, Herdegen T. The bright side of JNKs-Multitalented mediators in
605 neuronal sprouting, brain development and nerve fiber regeneration. Progress in neurobiology
606 2006;80(2):84-97.
607 46. Jardin I, Lopez JJ, Berna-Erro A, Salido GM, Rosado JA. Homer proteins in Ca(2)(+)
608 entry. IUBMB life 2013;65(6):497-504.
609 47. De Luca V, Annesi G, De Marco EV, et al. HOMER1 promoter analysis in Parkinson's
610 disease: association study with psychotic symptoms. Neuropsychobiology 2009;59(4):239-245.
611 48. van der Vaart B, Franker MA, Kuijpers M, et al. Microtubule plus-end tracking proteins
612 SLAIN1/2 and ch-TOG promote axonal development. The Journal of neuroscience : the official
613 journal of the Society for Neuroscience 2012;32(42):14722-14728.
614 49. Harripaul R, Vasli N, Mikhailov A, et al. Mapping autosomal recessive intellectual
615 disability: combined microarray and exome sequencing identifies 26 novel candidate genes in 192
616 consanguineous families. Molecular psychiatry 2018;23(4):973-984.
617 50. McGough IJ, de Groot REA, Jellett AP, et al. SNX3-retromer requires an evolutionary
618 conserved MON2:DOPEY2:ATP9A complex to mediate Wntless sorting and Wnt secretion.
619 Nature communications 2018;9(1):3737.
620 51. Zhao SB, Dean N, Gao XD, Fujita M. MON2 Guides Wntless Transport to the Golgi
621 through Recycling Endosomes. Cell structure and function 2020;45(1):77-92.
622 52. Lopes C, Chettouh Z, Delabar JM, Rachidi M. The differentially expressed C21orf5 gene
623 in the medial temporal-lobe system could play a role in mental retardation in Down syndrome and
624 transgenic mice. Biochemical and biophysical research communications 2003;305(4):915-924.

625 53. Rachidi M, Delezoide AL, Delabar JM, Lopes C. A quantitative assessment of gene
626 expression (QAGE) reveals differential overexpression of DOPEY2, a candidate gene for mental
627 retardation, in Down syndrome brain regions. International journal of developmental neuroscience
628 : the official journal of the International Society for Developmental Neuroscience 2009;27(4):393-
629 398.
630 54. Swaminathan S, Huentelman MJ, Corneveaux JJ, et al. Analysis of copy number variation
631 in Alzheimer's disease in a cohort of clinically characterized and neuropathologically verified
632 individuals. PloS one 2012;7(12):e50640.
633 55. Swaminathan S, Shen L, Kim S, et al. Analysis of copy number variation in Alzheimer's
634 disease: the NIALOAD/ NCRAD Family Study. Current Alzheimer research 2012;9(7):801-814.
635 56. Dergai O, Novokhatska O, Dergai M, et al. Intersectin 1 forms complexes with SGIP1 and
636 Reps1 in clathrin-coated pits. Biochemical and biophysical research communications
637 2010;402(2):408-413.
638 57. Drecourt A, Babdor J, Dussiot M, et al. Impaired Transferrin Receptor Palmitoylation and
639 Recycling in Neurodegeneration with Brain Iron Accumulation. American journal of human
640 genetics 2018;102(2):266-277.
641 58. Bagyinszky E, Youn YC, An SS, Kim S. The genetics of Alzheimer's disease. Clinical
642 interventions in aging 2014;9:535-551.
643 59. Lippa CF, Fujiwara H, Mann DM, et al. Lewy bodies contain altered alpha-synuclein in
644 brains of many familial Alzheimer's disease patients with mutations in presenilin and amyloid
645 precursor protein genes. The American journal of pathology 1998;153(5):1365-1370.
646 60. Deaton CA, Johnson GVW. Presenilin 1 Regulates Membrane Homeostatic Pathways that
647 are Dysregulated in Alzheimer's Disease. Journal of Alzheimer's disease : JAD 2020.

61. Gatto EM, Rojas GJ, Nemirovsky SI, et al. A novel mutation in PSEN1 (p.Arg41Ser) in an Argentinian woman with early onset Parkinsonism. Parkinsonism & related disorders 2020;77:21-25.

62. Ravanidis S, Bougea A, Papagiannakis N, et al. Validation of differentially expressed brain-enriched microRNAs in the plasma of PD patients. Annals of clinical and translational neurology 2020.

63. Abramzon YA, Fratta P, Traynor BJ, Chia R. The Overlapping Genetics of Amyotrophic Lateral Sclerosis and Frontotemporal Dementia. Frontiers in neuroscience 2020;14:42.

64. Doxakis E. RNA binding proteins: a common denominator of neuronal function and dysfunction. Neuroscience bulletin 2014;30(4):610-626.

65. Egorova PA, Bezprozvanny IB. Molecular Mechanisms and Therapeutics for Spinocerebellar Ataxia Type 2. Neurotherapeutics : the journal of the American Society for Experimental NeuroTherapeutics 2019;16(4):1050-1073.

66. Ravanidis S, Doxakis E. RNA-Binding Proteins Implicated in Mitochondrial Damage and Mitophagy. Frontiers in cell and developmental biology 2020;8:372.

67. Ravanidis S, Kattan FG, Doxakis E. Unraveling the Pathways to Neuronal Homeostasis and Disease: Mechanistic Insights into the Role of RNA-Binding Proteins and Associated Factors. International journal of molecular sciences 2018;19(8).

68. Salcedo-Arellano MJ, Dufour B, McLennan Y, Martinez-Cerdeno V, Hagerman R. Fragile X syndrome and associated disorders: Clinical aspects and pathology. Neurobiology of disease 2020;136:104740.

69. Kim JM, Hong S, Kim GP, et al. Importance of low-range CAG expansion and CAA interruption in SCA2 Parkinsonism. Archives of neurology 2007;64(10):1510-1518.

671 70. Wang C, Xu Y, Feng X, et al. Linkage analysis and whole-exome sequencing exclude extra
672 mutations responsible for the parkinsonian phenotype of spinocerebellar ataxia-2. Neurobiology
673 of aging 2015;36(1):545 e541-547.
674 71. Gwinn-Hardy K, Chen JY, Liu HC, et al. Spinocerebellar ataxia type 2 with parkinsonism
675 in ethnic Chinese. Neurology 2000;55(6):800-805.
676 72. Furtado S, Payami H, Lockhart PJ, et al. Profile of families with parkinsonism-predominant
677 spinocerebellar ataxia type 2 (SCA2). Movement disorders : official journal of the Movement
678 Disorder Society 2004;19(6):622-629.
679 73. Martens LH, Zhang J, Barmada SJ, et al. Progranulin deficiency promotes
680 neuroinflammation and neuron loss following toxin-induced injury. The Journal of clinical
681 investigation 2012;122(11):3955-3959.
682 74. Piscopo P, Grasso M, Fontana F, et al. Reduced miR-659-3p Levels Correlate with
683 Progranulin Increase in Hypoxic Conditions: Implications for Frontotemporal Dementia. Frontiers
684 in molecular neuroscience 2016;9:31.
685 75. Rademakers R, Eriksen JL, Baker M, et al. Common variation in the miR-659 binding-site
686 of GRN is a major risk factor for TDP43-positive frontotemporal dementia. Human molecular
687 genetics 2008;17(23):3631-3642.
688 76. Xu J, Xilouri M, Bruban J, et al. Extracellular progranulin protects cortical neurons from
689 toxic insults by activating survival signaling. Neurobiology of aging 2011;32(12):2326 e2325-
690 2316.
691 77. Yin F, Banerjee R, Thomas B, et al. Exaggerated inflammation, impaired host defense, and
692 neuropathology in progranulin-deficient mice. The Journal of experimental medicine
693 2010;207(1):117-128.

694 78. Bucher M, Fanutza T, Mikhaylova M. Cytoskeletal makeup of the synapse: Shaft versus
695 spine. Cytoskeleton 2020;77(3-4):55-64.
696 79. Pinho J, Marcut C, Fonseca R. Actin remodeling, the synaptic tag and the maintenance of
697 synaptic plasticity. IUBMB life 2020;72(4):577-589.
698 80. Rai SN, Dilnashin H, Birla H, et al. The Role of PI3K/Akt and ERK in Neurodegenerative
699 Disorders. Neurotoxicity research 2019;35(3):775-795.
700 81. Santo EE, Paik J. FOXO in Neural Cells and Diseases of the Nervous System. Current
701 topics in developmental biology 2018;127:105-118.
702 82. Junqueira SC, Centeno EGZ, Wilkinson KA, Cimarosti H. Post-translational modifications
703 of Parkinson's disease-related proteins: Phosphorylation, SUMOylation and Ubiquitination.
704 Biochimica et biophysica acta Molecular basis of disease 2019;1865(8):2001-2007.
705 83. Pajarillo E, Rizor A, Lee J, Aschner M, Lee E. The role of posttranslational modifications
706 of alpha-synuclein and LRRK2 in Parkinson's disease: Potential contributions of environmental
707 factors. Biochimica et biophysica acta Molecular basis of disease 2019;1865(8):1992-2000.
708 84. Calogero AM, Mazzetti S, Pezzoli G, Cappelletti G. Neuronal microtubules and proteins
709 linked to Parkinson's disease: a relevant interaction? Biological chemistry 2019;400(9):1099-1112.
710 85. Pellegrini L, Wetzel A, Granno S, Heaton G, Harvey K. Back to the tubule: microtubule
711 dynamics in Parkinson's disease. Cellular and molecular life sciences : CMLS 2017;74(3):409-
712 434.

713